BR69932

LEVEL II

ADA085033

ROYAL AIRCRAFT ESTABLISHMENT

14   TM

AERODYNAMIC CHARACTERISTICS OF MOVING TRAILING-EDGE CONTROLS

AT SUBSONIC AND TRANSONIC SPEEDS

by

D. G. Mabey

D. M. McOwat

B. L. Welsh

June 1979

DDC

RECEIVED
NOV 15 1979

B

ROYAL AIRCRAFT ESTABLISHMENT

AERODYNAMIC CHARACTERISTICS OF MOVING TRAILING-EDGE CONTROLS AT SUBSONIC AND TRANSONIC SPEEDS

by

D. G. Mabey

D. M. McOwat

B. L. Welsh

SUMMARY

This paper compares oscillatory pressures calculated and measured at high subsonic speeds for a swept back wing of aspect ratio 6 with a part-span trailing-edge flap. The flap was driven at frequencies of 1 Hz (quasi-steady) and 90 Hz at Mach numbers from 0.40 to 0.95 with both fixed and free transition over a range of Reynolds numbers from 10^6 to 4×10^6.

The measured oscillatory pressures depend strongly on the boundary-layer displacement thickness at the hinge line. Hence extrapolation from model to full scale requires great care. In subsonic flow, tests with free transition give the thinnest turbulent boundary layer at the hinge line and come nearest to full scale. However, at transonic speeds transition should be fixed at a safe distance upstream of the most forward excursion of the shock wave to obtain results appropriate to higher Reynolds number.

Tests with flap driven simultaneously at two frequencies (90 Hz and 131 Hz) at subsonic and transonic speeds produce the same oscillatory pressures at 131 Hz as when driven independently. Hence the principle of superposition applies, at least for small amplitude motions with attached flows.

LIST OF CONTENTS

1 INTRODUCTION

The effective use of active controls for load alleviation or flutter suppression requires a better knowledge of the dynamic characteristics of aerodynamic controls than is currently available, for even at subsonic speeds wide differences frequently occur between calculations and measurements in wind tunnels. As an example, Fig 1 shows some measurements[1] of the total dynamic lift induced by an oscillating flap on a low aspect ratio wing. The total lift was measured with a dynamic balance fully described in Ref 2. The lift derivative in phase with the motion (z_β) is only about 60% of that predicted by the linear theory of Ref 3 over the Mach number range from M = 0.6 to 0.9. The measured lift in quadrature with the motion (z_β') does not even have the trend with Mach number predicted by the theory. Fig 2 shows similar evidence for the pitching moment. The position with regard to the flap hinge moment is even more unsatisfactory. Fig 3 shows that the hinge moment in phase with the motion ($-h_\beta$) decreases with Mach number, whereas the theory predicts an increase. In contrast, the hinge moment in quadrature with the motion ($-h_\beta'$) shows the correct trend against Mach number, but is only about 60% of that predicted. These anomalies on a simple configuration of 5% thickness/chord ratio were tentatively explained in Ref 1 in terms of a semi-empirical correction for aerofoil section and boundary layer effects together with a correction for wall interference. However both corrections were restricted to low frequency and to subcritical flow and would not be applicable to other configurations. Similar anomalies have been cited previously on a number of aerofoils, the measured forces being about 70% of those predicted[4]. For aerofoils the anomalies discussed are often attributed to the omission of wing and boundary layer thickness from the calculations and when these thicknesses are included some improvement is achieved[4]. However no direct experimental evidence for thickness and boundary layer effects has yet been adduced for wings with oscillating controls.

To provide clear evidence of the importance of boundary layer thickness, and to highlight the uncertainties in the linearized theories at transonic speeds and moderately high frequencies, an extensive series of oscillatory pressure measurements has been made, with both fixed and free transition, on a half model of a swept wing of aspect ratio 6 with a trailing-edge flap (Fig 4). This symmetric wing 9% thick (RAE Wing A) was tested mainly at zero incidence. For a wing of this type an understanding of the unsteady flow and how it is affected by Reynolds number is likely to be important in the design of an active control system. This paper provides a preview of some of the more interesting results from the experiments; a full account will be published later[5].

2 EXPERIMENTAL DETAILS

2.1 Pressure measurements

Fig 4 shows the position of the four spanwise stations used for the pressure measurements, and the flap.

The oscillatory pressures were measured by small transducers (Kulite type XCQL 093-25A) mounted close to the pressure holes to ensure only small changes in the amplitude and phase. With the installation used amplitude errors are estimated to be less than 1.5% and phase errors less than 1.5°, for the highest test frequency (131 Hz). The steady pressures were measured in a separate test in the traditional way by connecting the static pressure holes through long lengths of piping to manometers outside the tunnel. With new amplifiers developed at RAE[6] the same pressure transducers can now measure both dynamic and static pressure distributions simultaneously.

2.2 Model construction

The method of construction was unusual. The model was made in two halves to allow access to the pressure transducers and to the drive shaft of the flap (Fig 5). These halves were then screwed together and produced a flexible model, which responded to the flow unsteadiness in the tunnel when the flap was undriven. The structural response was a minimum at 90 and 131 Hz and so these frequencies were selected for driving the flap. Nevertheless the flap inertia and the aerodynamic loads developed by the flap forced significant wing deflections, which were determined by internal miniature accelerometers. Typical values of the amplitudes of these deflections are: 2 mm at the wing tip and 0.2° twist. No corrections have yet been made to the measured oscillatory pressures for these wing motions, although in principle this should be possible. When active control systems are used in flight similar dynamic wing deflections may occur because aircraft are relatively flexible - as illustrated by well known static aeroelastic phenomena such as aileron reversal and wing divergence.

2.3 Boundary layer measurements

A novel method was used to estimate the boundary layer displacement thickness, δ_1, just upstream of the flap hinge line. Instead of making measurements of the boundary layer profile, at several stations on the wing, the local skin friction was inferred from the reading of a single Preston tube of diameter 1 mm just upstream of the flap hinge line and inboard of the flap (Fig 4). The skin friction coefficient, C_f, was computed using the method of reference 7; a probe correction of 0.15 x probe diameter was applied to the distance from the aerofoil surface to the centre of the Preston tube. The boundary layer Reynolds number based on the displacement thickness δ_1, $R\delta_1$, was inferred from the C_f-$R\delta_1$, relation derived from a viscous three-dimensional flow calculation made by Roberts[8]. This calculation showed (Fig 6) that on the hinge line at M = 0.40 there was

a unique relation between C_f and R_{δ_1}, both inboard of the flap (at $\eta = 0.28$) and outboard of the flap (at $\eta = 0.80$). The calculations also showed that C_f at the hinge line only increased a little with the rearward movement of the transition point from $x_t/c = 0.125$ to 0.25. Hence the same curve could be used to make rough estimates of the boundary-layer thickness at the hinge line for transition-free measurements. Fig 6 shows that the predicted C_f's are appreciably lower than the corresponding two-dimensional flat plate C_f's. This is because of the change in boundary-layer profile due to the small adverse pressure gradient towards the rear of the aerofoil. The insert in Fig 6 shows that at a typical station the measured and calculated viscous pressure distributions are in good agreement, despite the unusual method of construction of the model, which involves a discontinuity at the leading-edge and a trailing-edge of small thickness.

The shape of the pressure distribution remains essentially unchanged in character from M = 0.40 to 0.85 so that Fig 6 should be quite adequate to estimate comparative variations in boundary layer thickness at subsonic speeds. The change in the character of the pressure distribution at transonic speeds prevents Fig 6 from being used to estimate the boundary layer thickness at the hinge line at M = 0.90 and 0.95. However, predictions from a viscous transonic flow calculation by Firmin for M = 0.90 have recently become available[9], and these have been used to indicate the probable magnitude of the boundary layer thickness, although the predicted skin friction coefficients are appreciably lower than the measurements (Fig 12).

2.4 Test conditions

The model was mounted on the sidewall of the RAE 3ft x 3ft tunnel and tested over the Mach number range from M = 0.40 to 0.95 in the top and bottom slotted section (0.91 m wide x 0.64 m high). Table I lists the Reynolds numbers and boundary layer thicknesses for the oscillatory pressure measurements cited here, and gives typical full scale values.

TABLE I

Standard Test Conditions $p_t = 0.95$ bar		
Mach Number	Reynolds Number	Boundary Layer Thickness
M	$10^{-6} \times Rc_o$	$10^3 \, \delta_1/c_o$
		Free / Fixed
0.65	2.8	1.7 / 2.9
0.80	3.1	2.3 / 3.7
Predicted values 0.90	3.3	– / 3.9
Typical full scale values		
0.80	120.0	0.7 / –

The other tunnel total pressures, p_t, were 0.24, 0.47 and 1.52 bar, giving Reynolds numbers in the range from $Rc_o = 10^6$ to 6×10^6. The roughness band was formed by a thin steel strip 1.6 mm wide glued at x/c = 0.05 on both surfaces of the wing. The steel strip was indented by a pyramidically pointed needle to give "coronets" 0.13 mm high 2 mm apart. This roughness was judged to be as effective as a distribution of spheres of 0.13 mm diameter, and could be applied more readily and repeatably.

3 RESULTS

Fig 7 shows that although the wing flow at $\alpha = 0^\circ$ is three-dimensional, the local Mach number contours are swept and straight for two typical free-stream Mach numbers. M = 0.80 (subsonic) and M = 0.90 (transonic). The flow for M = 0.80 is just subcritical, the maximum local Mach number $M_e = 0.96$, occurring near quarterchord, while M = 0.90 introduces supersonic flow over half the wing and a peak value of about $M_e = 1.20$ in the region of 35% chord. After consideration of the measured and calculated oscillatory pressure distributions, the role of transition fixing and the influence of the boundary layer is discussed.

3.1 Comparisons with theory

Fig 8 shows a typical comparison of the measured chordwise oscillatory pressure distributions with fixed transition at four spanwise positions for M = 0.80 with predictions according to an inviscid linearised theory for three-dimensional flow, developed by Marchbank[10]. These measurements are conveniently represented by the magnitude of the vector, C_p/δ, and the phase angle ϕ relative to the movement of the flap.

On the control (at $\eta = 0.45$ and 0.60) the magnitude, C_p/δ, in Fig 8a is large close to the hinge line and agrees well with the linearised theory as far as 75% chord; aft of this the aerofoil thickness and the boundary layer combine to lower the loading. Just inboard of the control at $\eta = 0.35$ the magnitudes are much smaller but still in good

agreement with the predictions. In contrast, just outboard of the control at $\eta = 0.75$ the magnitudes remain fairly high. However the measurements show anomalous variations from 10% to 40% chord which are not in accord with the predictions and which are tentatively attributed to a small laminar separation bubble[5].

The phase angle of the pressures in Fig 8b shows an interesting variation from section to section. Over the span of the control the measured phase angles lag appreciably behind the predictions, and this must be attributed to the lag effects associated with the higher local velocities caused by the wing thickness. However, just off the control the measured phase angles actually lead the predictions.

More complex and interesting spanwise variations develop at transonic speeds, which are discussed elsewhere[5]. No theoretical calculations of the oscillatory flow are currently available for supercritical flow conditions.

Fig 9 shows another comparison at $M = 0.65$ and $\eta = 0.60$ for two flap amplitudes of $0.5°$ and $2°$ at a frequency of 90 Hz. Flap amplitude has only a small influence on C_p/δ and a negligible influence on the phase angle. Upstream of $x/c = 0.6$ the measured C_p/δ is in excellent agreement with the predictions, but there are minor deviations close to the hinge line. The measured phase angles lag about $10°$ behind those predicted, just as at $M = 0.80$, and may again be attributed to the higher local Mach numbers due to wing thickness.

3.2 Principle of superposition

For active control technology it is important to know the limits of linearity of the pressures induced by control displacement, because these limits determine the region within which the principle of superposition is valid. Fig 10 illustrates some results of a brief preliminary investigation of this question at subsonic and transonic speeds with fixed transition.

With regard to the superposition of different flap frequencies at subsonic speeds, Fig 10a shows the chordwise variation of the oscillatory pressures at $\eta = 0.45$ (Section 2 of Fig 4); the content of oscillatory pressures at 131 Hz is virtually unchanged when a flap oscillation amplitude of $1°$ at 90 Hz is added to one of amplitude $1°$ at 131 Hz. Thus the results shown in Figs 9 and 10a and similar tests at $M = 0.80$, confirm that the principle of superposition is valid at subsonic speeds, at least within this restricted range of amplitudes and frequencies.

Fig 10a includes predictions for the higher frequency. The magnitude of the vector is now only in agreement with the predictions upstream of $x/c = 0.4$ (cf $x/c = 0.6$ for the lower frequency in Fig 9), the phase angles measured now lag about $10°$ to $20°$ behind those predicted. Thus at the higher frequency the predictions are somewhat less satisfactory, and the phase difference between the measurements and the predictions is roughly proportional to the frequency parameter.

Only a limited test of the principle of superposition was made at transonic speeds. Fig 10b shows the chordwise variation of the oscillatory pressures at $\eta = 0.45$; the frequency content of the oscillatory pressures at 131 Hz is hardly changed when a flap oscillation of amplitude $1°$ at 90 Hz is added to one of amplitude $1°$ at 131 Hz, just as at the subsonic speed.

3.3 Transition measurements

The boundary-layer transition position for $\eta = 0.60$ was inferred from the movements of peaks in the surface pressure fluctuations with tunnel total pressure, p_t, when the flap was undriven. On flat plates and cones this method reveals a peak in the broad-band pressure fluctuations of about $p/q = 1.0\%$ in the middle of the transition region[11], where rapid local changes in thickness occur within the boundary layer. On a wing the mean pressure gradients at subsonic speeds, and shock waves at transonic speeds, make the interpretation of the surface pressure fluctuation measurements more difficult. This difficulty can be partially overcome by using the local kinetic pressure, q_e, as a reference. Moreover comparison of transition free and transition fixed results generally eliminates any ambiguities. Fig 11 shows some typical transition-free measurements. At $M = 0.80$, Fig 11a shows two well-defined peaks, indicating transition just forward of the hinge line at the lower total pressure $p_t = 0.24$ and 0.47 bar. At the higher pressures, $p_t = 0.95$ and 1.52 bar, the peaks occur at about 40% chord. By comparison with the transition-fixed measurements, we may infer that transition is roughly about 30% chord. In contrast, at transonic speeds Fig 11 shows well-defined high peaks at all pressures. These peaks are caused by the oscillation of the shock terminating the local supersonic region. Initially the peaks and the shock wave/boundary layer interaction move forward as p_t increases because the transition front moves forward as the Reynolds number increases. (In contrast, with transition fixed close to the leading-edge a shock wave would generally move slowly downstream as Reynolds number increases). The large peak pressure fluctuations at the lower pressures ($p_t = 0.24$ to 0.95) indicate laminar shock wave/boundary layer interactions. The smaller peak pressure fluctuation at the higher pressures ($p_t = 1.52$ bar) indicates a turbulent shock wave/boundary layer interaction of more limited extent. Laminar interactions are, of course, much longer than turbulent interactions and therefore are more likely to create large peak pressure fluctuations. A similar change in peak p/q in going from a laminar to a turbulent interaction was also reproduced at lower total pressures transition fixed (omitted here for brevity). Hence at transonic speeds the variation of peak pressure

fluctuations with Reynolds number can be a valuable guide to the state of the boundary layer at the shock even though it cannot give the precise transition position.

With the roughness band at the standard test pressure (p_t = 0.95 bar), transition was always close to the leading-edge so that the boundary layer at the hinge line was excessively thick relative to full-scale values. Hence from the point of view of the trailing-edge flap, the boundary layer at the standard pressure must be described as "overfixed", with all the difficulties that this condition is known to introduce for steady measurements. (See for example the discussion in Refs 12 and 13).

3.4 Skin friction measurements

Fig 12 shows the local skin friction coefficients derived from the Preston tube readings as a function of the Reynolds number based on the root chord. It is convenient to consider first the Mach number range from M = 0.40 to 0.90. Here the skin friction measurements with both free and fixed transition all fall monotonically with Reynolds number. This shows that the boundary layer is always turbulent at the hinge line, even at the lowest Reynolds number. This inference is consistent with the transition measurements. The skin friction is always significantly higher with transition free than with transition fixed, confirming that the transition free boundary layer is appreciably thinner at the hinge line and more representative of full scale flow over the control surfaces.

The transition fixed skin friction measurements at M = 0.40 may be compared directly with the estimates given by Roberts[8]. For the higher Reynolds number ($Rc_0 > 10^6$) the measured transition fixed skin friction coefficients are about 3% lower than the estimates, consistent with a thicker boundary layer. This is because at these high Reynolds numbers natural transition is close to the roughness band at x/c = 0.05 whereas the estimates assume a transition position further downstream at x/c = 0.125. In marked contrast, at the lower Reynolds numbers ($Rc_0 < 10^6$), the measured skin friction coefficients with fixed transition are appreciably higher than the estimates, consistent with transition moving progressively further downstream of x/c = 0.125 as Reynolds number decreases and with the roughness band becoming less effective. A rearward movement of transition at low Reynolds numbers would significantly increase the local skin friction at the measurement station, according to the estimates[8] included in Fig 12.

The skin friction measurements at M = 0.95 are included in Fig 12 to illustrate the dangers inherent in making aerodynamic measurements at transonic speeds with transition free. As the Reynolds number increases, the skin friction first increases and then decreases rapidly as mean position of the shock alters. In marked contrast, with transition fixed the skin friction coefficient decreases monotonically with Reynolds number, just as at the lower Mach numbers. This is consistent with relatively minor movements of the shock wave around x/c = 0.50 and with appreciable variations in boundary layer thickness. For this wing, at M = 0.95 and zero incidence, it would have clearly been preferable to fix transition with a roughness band at, say, x/c = 0.3 rather than at x/c = 0.05.

Fig 13 shows the variation of the ratio of the boundary layer displacement thickness at the Preston tube to the root chord, δ_1/c_0, with Mach number and Reynolds number both with transition free and fixed.

Considering first the measurements at M = 0.40, we see that with transition free the boundary layer thickness ratio increases monotonically with Reynolds number while the transition point moves progressively further upstream. In contrast, with transition fixed the boundary layer thickness ratio initially increases rapidly with Reynolds number as the roughness initiates transition and rapidly moves the transition front close to the roughness band[14]. Further increase in Reynolds number then slowly decreases the boundary layer thickness ratio. At the standard test pressure, p_t = 0.95 bar, the displacement thickness of the boundary layer is 50% thicker with transition fixed than with transition free. The predictions by the three-dimensional viscous flow calculations show that a boundary layer thickness ratio appropriate to a full-scale Reynolds number of 120 x 10^6 (δ_1/c_0 = 0.0007) could have been achieved with transition free at a greatly reduced Reynolds number of 0.6 x 10^6. Although it is not suggested that this method of simulation would be entirely adequate, it should be worth a more detailed investigation in future tests, in view of the strong influence of boundary layer thickness on pressure measurements for oscillating trailing-edge flaps.

The results at higher speeds are similar in character to those at M = 0.40, with the boundary layer thickness ratio increasing with Mach number, presumably because of the increasing adverse pressure gradient at the rear of the wing. The important point to notice from Fig 13 is that a marked difference in boundary layer thickness ratio is maintained between transition free and transition fixed measurements at all Reynolds numbers.

3.5 Influence of boundary layer

We now consider the influence of the boundary layer on the oscillatory pressures measured across the chord of a typical spanwise section n = 0.60 (Section 3 of Fig 4).

In general, with the thin turbulent boundary layer at the hinge line allowed by free transition, the flap lift curve slope is significantly increased relative to the case with the thick turbulent boundary layer formed with fixed transition. Thus at M = 0.40, the increase in flap lift curve slope produces a significant increase in the near load of the oscillatory pressures measured over the whole section. A similar increase was expected and observed in the quasi-steady measurements. However in addition with the thinner

boundary layer there is a significant increase (about 6°) in the phase lag of the oscillatory pressures over the forward portion of the section, whereas over the central portion this increase is only about 3°. This change in phase angle was unexpected and is more difficult to explain than the increase in the magnitude of the vector. Moore's review[15] of the limited information available in 1969 on the scale effects on control-surface derivatives suggested that with a thinner boundary layer (obtained either by increasing Reynolds number or by allowing free transition), stiffness derivatives increased but damping derivatives were unaltered. Thus, as in the present measurements, the magnitude of the force vector was increased but there was a decrease in phase lag contrary to the present measurements. Moore concluded that, to obtain results closest to full-scale values, tests with oscillating trailing-edge controls were best made transition free. The change in phase angle is unlikely to be caused by the small differences in the distributions of Mach number in the mean flow between transition fixed and free. In a rough attempt to quantify the effect of these small differences, Tijdeman's two-dimensional acoustic wave formula[16] was used to estimate the equivalent phase lag for a source mounted at the hinge line. The relaxation factor assumed was 0.7, as Tijdeman found appropriate for an oscillating wing, but essentially similar results would have been found with a relaxation factor of 1.0. The dotted curve in Fig 14 shows that the differences between the predicted phase lags with transition fixed and free are negligible. However, the phase lags predicted are much larger than those measured, so that the two-dimensional acoustic theory is plainly inappropriate for this three-dimensional situation, although it suggests that the large change in phase angle may be a dynamic phenomenon within the boundary layer.

Now at any given subsonic Mach number and Reynolds number (ie for a very wide range of transition positions) the same trends occur as those illustrated in Fig 14. Hence the viscous phenomena influencing the changes in both magnitude and phase angle are probably determined by the thickness of the turbulent boundary layer at the hinge line, rather than the influence of the laminar portion of the boundary layer upstream of transition.

Fig 14 also includes the predictions according to linearised theory[10]. Generally the magnitude of the vector is well predicted. Although upstream of x/c = 0.60 the predictions are in better agreement with the measurements made with transition fixed rather than with transition free, this should be considered fortuitous, because the theory takes no account of wing or boundary layer thickness. Close to the hinge line the predictions are, in fact, in better agreement with the measurements made transition free. It is important to recall that at x/c = 0.30 the local Mach number is 0.96, so that such good agreement is really surprising.

As regards phase angles the theory predicts an oscillatory pressure at x/c = 0.05 which lags by about 50°. The pressure observed lags by about 60°. Similar discrepancies in phase angle are observed right across the section and must be attributed to the higher local velocities caused by the wing thickness.

When the wing flow is transonic, the pressures produced by oscillation of the flap are dominated by the type of shock wave/boundary layer interaction (Fig 15). Thus at M = 0.90, when transition is free, we have seen that the shock wave/boundary layer interaction is laminar and extends over a long portion of the chord (say from x/c = 0.3 to 0.6). The interaction causes large oscillatory pressures in this region in addition to the large oscillatory pressures which would be expected in the subsonic portion of the flow field close to the hinge line. In marked contrast, with fixed transition the oscillatory pressures associated with the shock are somewhat smaller and concentrated about the mean shock position at x/c = 0.3. Downstream of the turbulent shock wave/boundary layer interaction the oscillatory pressures first fall rapidly and then increase towards the hinge line. The magnitude of this increase is quite small until the hinge line is approached, and its character resembles that observed in the same region at M = 0.8 (cf Fig 14). The measurements suggest that the flap lift slope is still appreciably higher with the thin turbulent boundary layer produced by free transition. In addition we notice that there is once again a significant change in phase angle, for upstream of x/c = 0.5 the transition free measurements lag behind those with transition fixed by about 10° to 20°. This lag is in the same sense as that observed at subsonic speeds (Fig 14). This again suggests that the lag is not primarily caused by a changed mean flow, but by a dynamic phenomenon associated with the significant change in the boundary layer thickness. The lack of agreement of these measurements made with transition fixed and free suggests that for transonic speeds transition should always be fixed a safe distance upstream of the maximum forward excursion of the oscillatory shock wave, rather than close to the leading-edge, in an attempt to obtain aerodynamic characteristics appropriate to higher Reynolds number. Thus in Section 3.4 above it was suggested that at M = 0.95, with the shock at x/c = 0.5, transition should have been fixed at x/c = 0.30, rather than at x/c = 0.05.

Boundary-layer thickness is likely to have a much greater influence on the characteristics of a trailing-edge flap on a thick supercritical wing, particularly when this operates close to separation. Hence, when testing supercritical wings with oscillating trailing-edge flaps, some boundary layer thickness variation should always be included as an aid to the assessment of full scale performance.

4   FUTURE RESEARCH

The results already obtained on this model are judged to be of sufficient interest to justify a further investigation, particularly of the effects of changes in the boundary layer.

8

One shortcoming of the present tests is that the pressures were not measured close enough to the trailing edge (eg Figs 9 and 14). Hence the aluminium alloy flap has now been replaced with a stiffer flap (Fig 16) made in carbon fibre with 12 instead of 6 pressure orifices. This flap will be driven electromagnetically at higher frequencies and at larger amplitudes. (From about 20° at 25 Hz to 1^O at 200 Hz). The flap amplitude will be more precisely determined with a new type of fibre-optic instrument mounted on the drive shaft[17]; this instrument has no significant errors up to frequencies as high as 500 Hz.

Although the results for the tests of superposition are, of course, only established for attached flows, they suggest a useful interim practical application of active control technology to reduce the model response to unsteadiness in the tunnel flow. The model is flexible and responds strongly at the fundamental wing bending frequency (about 60 Hz). During the next series of tests the pressures induced by small amplitude flap oscillations at this frequency will be measured, the corresponding phases and amplitudes of all the wing accelerometers will be noted. These "open loop" measurements will then be used to formulate a suitable "closed loop" control law relating one of the accelerometer responses to an appropriate flap movement to reduce the wing responses and thus extend the fatigue life of the model. Ultimately we intend to extend our measurements of flap effectiveness to conditions of fully separated flow when there is significant buffeting.

5   CONCLUDING REMARKS

On this 9% thick symmetric wing the boundary layer has a large effect on the pressures generated by the oscillating trailing-edge flap, even at zero lift. With the thin turbulent boundary layer at the hinge line allowed by natural transition the flap produces appreciably higher forces at subsonic speeds, as was confirmed by the quasi-steady measurements. However, the increase in phase lag with the thinner boundary layer was not expected and has not yet been explained.

It is essential at transonic speeds to ensure a turbulent shock wave/boundary layer interaction, even in the absence of separation. Ideally the turbulent boundary layer should be as thin as possible. This may be achieved either by fixing transition just upstream of the shock, or by increasing the Reynolds number just until a turbulent shock wave/boundary layer interaction is obtained with free transition.

Although the effects of the boundary layer and wing thickness are not included, the predictions from lifting surface theory provide fair overall agreement with the measurements at subsonic speeds particularly at frequency parameters up to about 0.4. The authors hope that the present measurements at transonic speeds, and those yet to be made, will serve as a challenge to theoreticians to develop adequate theories for this difficult speed range.

NOTATION

C_p/δ	magnitude of vector of oscillatory pressure per radian flap deflection
C_f	local skin friction coefficient
c, $\bar{c}$, c_o	local, average, and root chords
f	freqeuncy (Hz)
h_β , $h_{\dot{\beta}}$; m_β , $m_{\dot{\beta}}$; $z_{\dot{\beta}}$, z_β	respectively hinge moment, pitching moment and lift derivatives in phase and in quadrature with flap displacement (Ref 1)
M	Mach number
p_o	tunnel total pressure
$\bar{p}$	rms pressure fluctuations
q	kinetic pressure
R	unit Reynolds number
U	stream velocity
x	streamwise distance from local leading-edge
α	angle of incidence
β	flap deflection in streamwise plane (radians, Ref 1)
δ	flap deflection normal to hinge line (radians, unless otherwise stated)
δ_1	boundary layer displacement thickness
η	spanwise distance as a fraction of semi-span
ϕ	phase of pressure oscillation relative to flap motion (deg positive for pressure leading displacement)
ν	frequency parameter $= 2\pi f\bar{c}/U$

Subscripts

e	local external flow conditions
t	transition position

10

REFERENCES

1   N C Lambourne, K C Wight, B L Welsh. Measurement of control surface oscillatory
     derivatives on a swept back, tapered model wing in two transonic tunnels.
     R&M 3806 1976.

2   K C Wight, N C Lambourne. A control surface oscillatory derivative rig for use
     with half models in high speed wind tunnels. ARC CP 1353 1975.

3   D E Davies. Calculation of unsteady generalised airforces on a thin wing
     oscillating harmonically in subsonic flow. R&M 3409 1963.

4   H Tijdeman. High subsonic and transonic effects in unsteady aerodynamics.
     NLR TR 750790 May 1975.

5   D McOwat, B L Welsh, B Cripps. Time-dependent pressure measurements on a swept
     wing with an oscillating flap at subsonic and transonic speeds.
     RAE TR in preparation.

6   B L Welsh, C R Pyne. A method to improve the temperature stability of semi-
     conductor strain gauge pressure transducers. RAE TR 77155, October 1977.

7   J M Allen. Use of the Baronti-Libby transformation and Preston tube calibrations
     to determine skin friction from turbulent velocity profiles. NASA TNP 4853
     November 1968.

8   A Roberts. The spline-Neumann system: comparison of experimental results for W4
     with a preliminary boundary layer treatment. BAC Aero Report 34 1977.

9   M Firmin. Private Communication, December 1978.

10   W R Marchbank. Evaluation of pressure distribution on thin wings with distorted
     control surfaces oscillating harmonically in linearised compressible subsonic
     flow. R&M 3783 1978.

11   D G Mabey. Boundary layer transition measurements on the AEDC 10° cone in three
     RAE wind tunnels and their implications. R&M 3821 1978.

12   J F Cahill. Simulation of full scale flight aerodynamic tests in existing transonic
     tunnels. Paper C20, AGARD CP 83-71 April 1971.

13   A B Haines. Further evidence and thoughts on scale effects at high subsonic speeds.
     Paper 43, AGARD CP 174 October 1975.

14   E L Van Driest. Boundary layer transition at supersonic speeds. Three-dimensional
     roughness effects (spheres). Jn Aero Space Sci Vol 29, p 909, August 1962.

15   A W Moore. Scale effects on oscillatory control - surface derivatives.
     ARC CP 1151 1971.

16   H Tijdeman. Investigations of the transonic flow around oscillating aerofoils.
     NLR TR 77090U October 1977.

17   B L Welsh. A new angular displacement transducer. RAE TR 79-026.
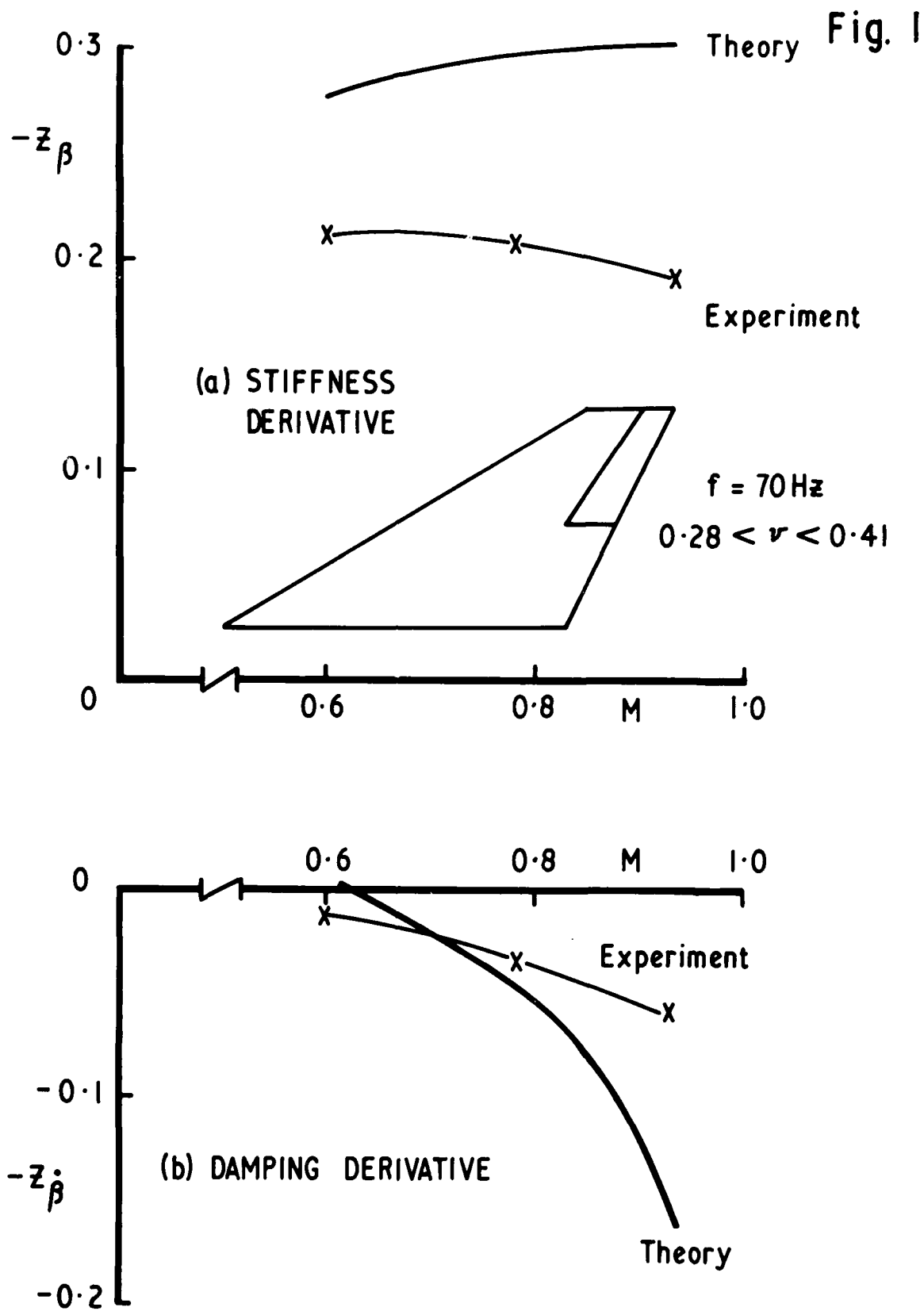
Fig. 1

$-z_\beta$

0.3

0.2

Theory

X   X   X

Experiment

(a) STIFFNESS DERIVATIVE

0.1

$f = 70\,Hz$

$0.28 < \nu < 0.41$

0   0.6   0.8   M   1.0

0.6   0.8   M   1.0

0

X   X   X

Experiment

-0.1

(b) DAMPING DERIVATIVE

$-z_{\dot\beta}$

Theory

-0.2

**Fig. 1   Lift Due to Oscillating Flap
v Mach Number**

Fig. 2

(a) STIFFNESS DERIVATIVE

$f = 70\,Hz$

$0.28 < r < 0.41$

Pitching Axis

(b) DAMPING DERIVATIVE
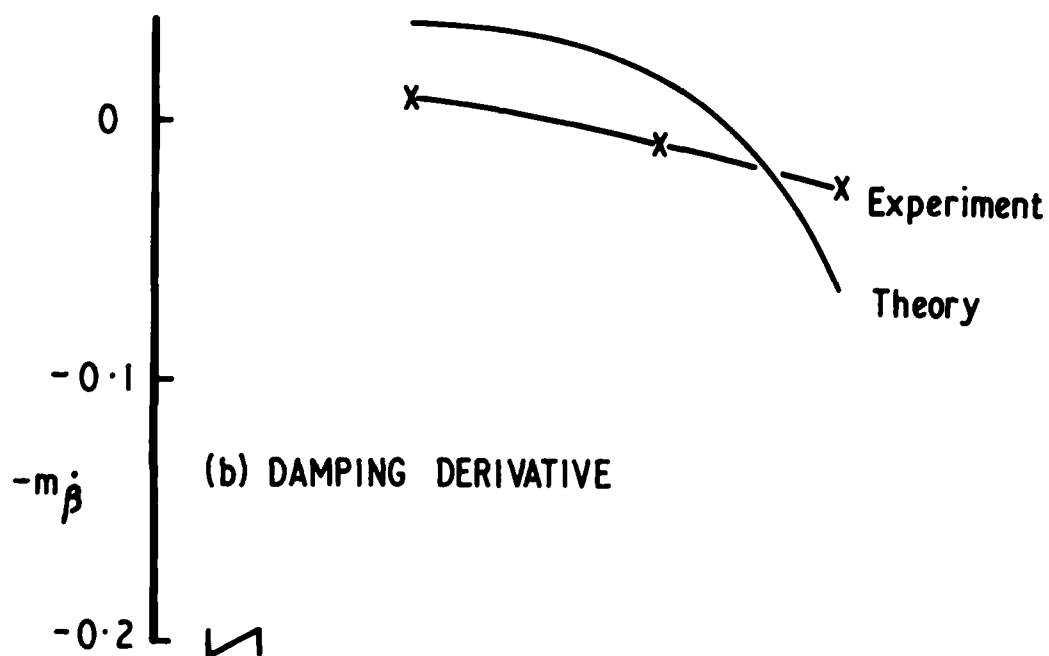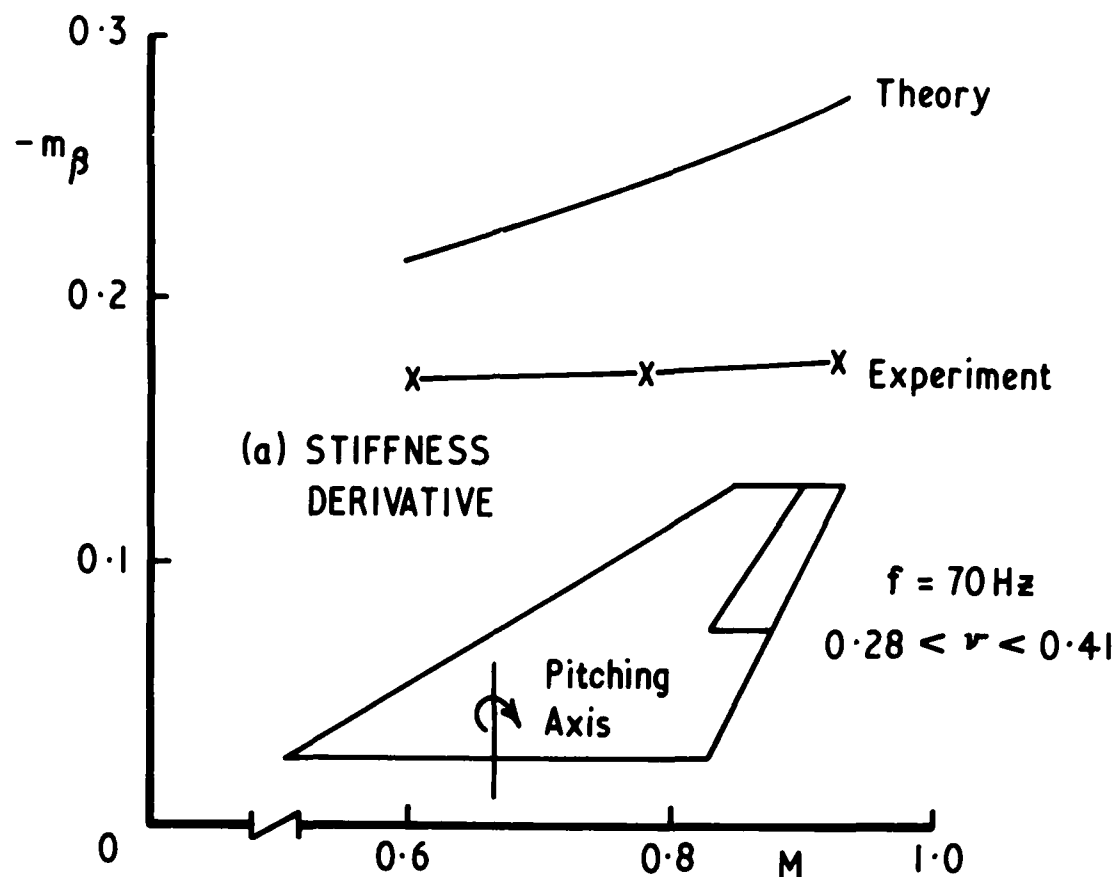
Fig. 2 Pitching Moment Due to Oscillating
Flap v Mach Number

Fig. 3

$f = 70 \, Hz$

$0.28 < \nu < 0.41$

(a) STIFFNESS DERIVATIVE

(b) DAMPING DERIVATIVE
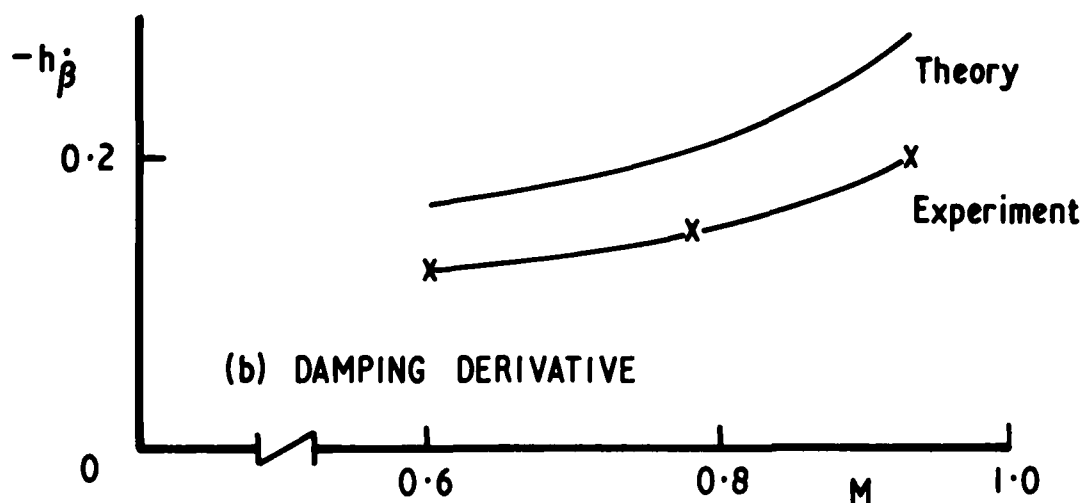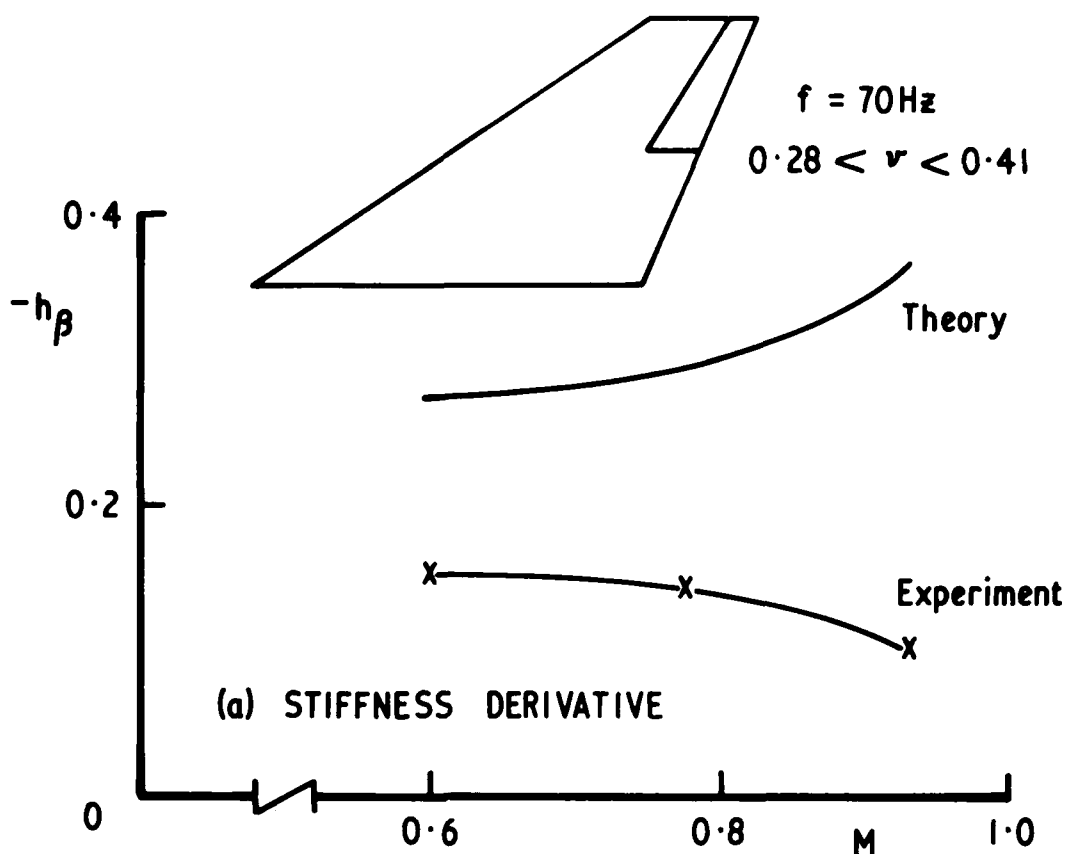
Fig. 3 Hinge Moment Due to Oscillating
Flap v Mach Number

Fig. 4

9% RAE 101 Section
Aspect Ratio 6
Taper Ratio 1/3
$\bar{c}$ = 0.160m
Area = 0.168m²

x/c = 0.70
Hinge Line

η
1.00

Section 4 — — — — 0.75
0.70

Section 3 — — — — 0.60

Section 2 — — — — 0.45
0.40

Section 1 — — — — 0.35

Preston Tube

36.7°   30°   22.3°

c_0 = 0.240m

T Memo Struct 947

Fig. 4   RAE Wing A

Fig 5

Leading – Edge

Trailing – Edge

Flap

Drive Shaft
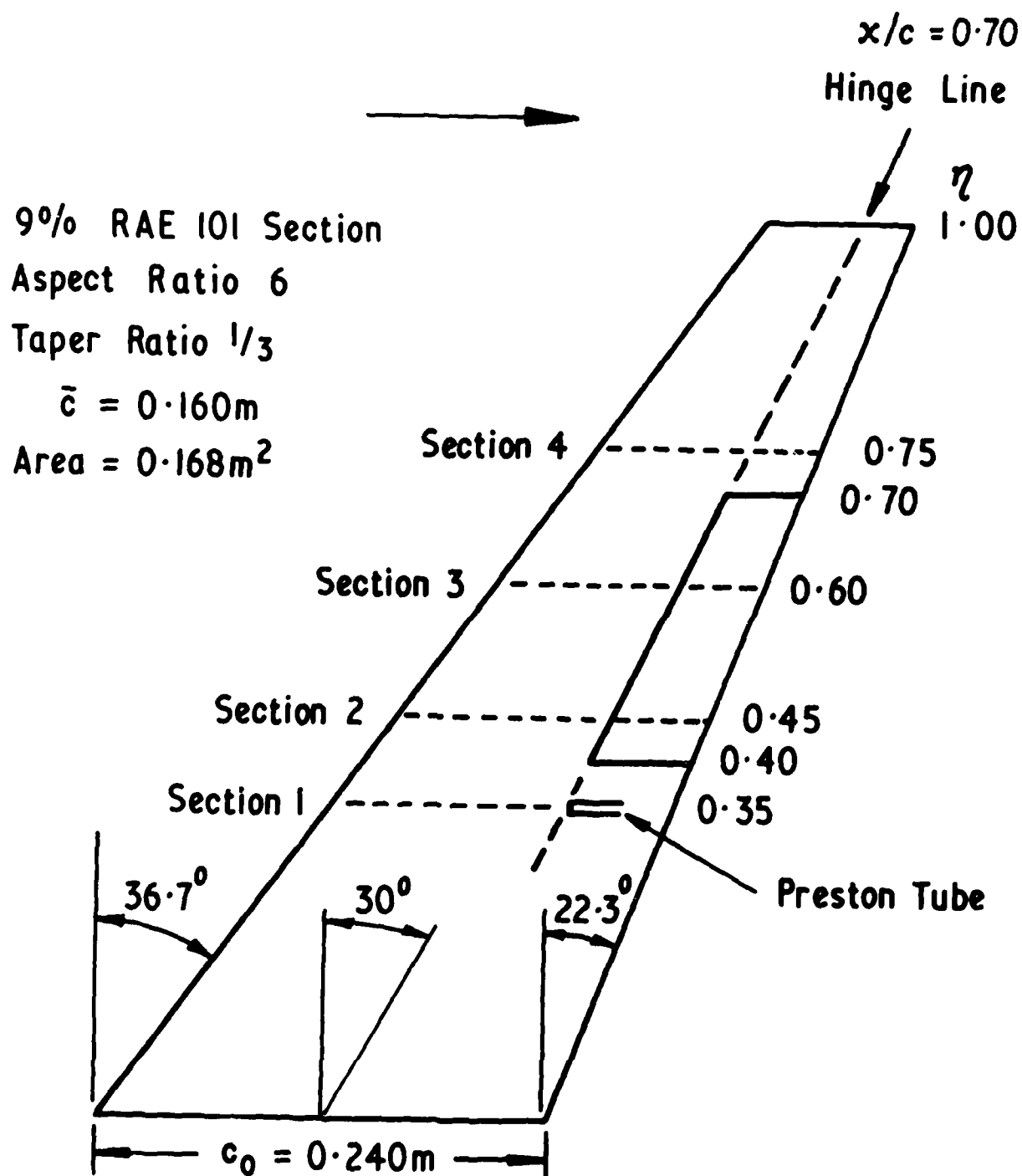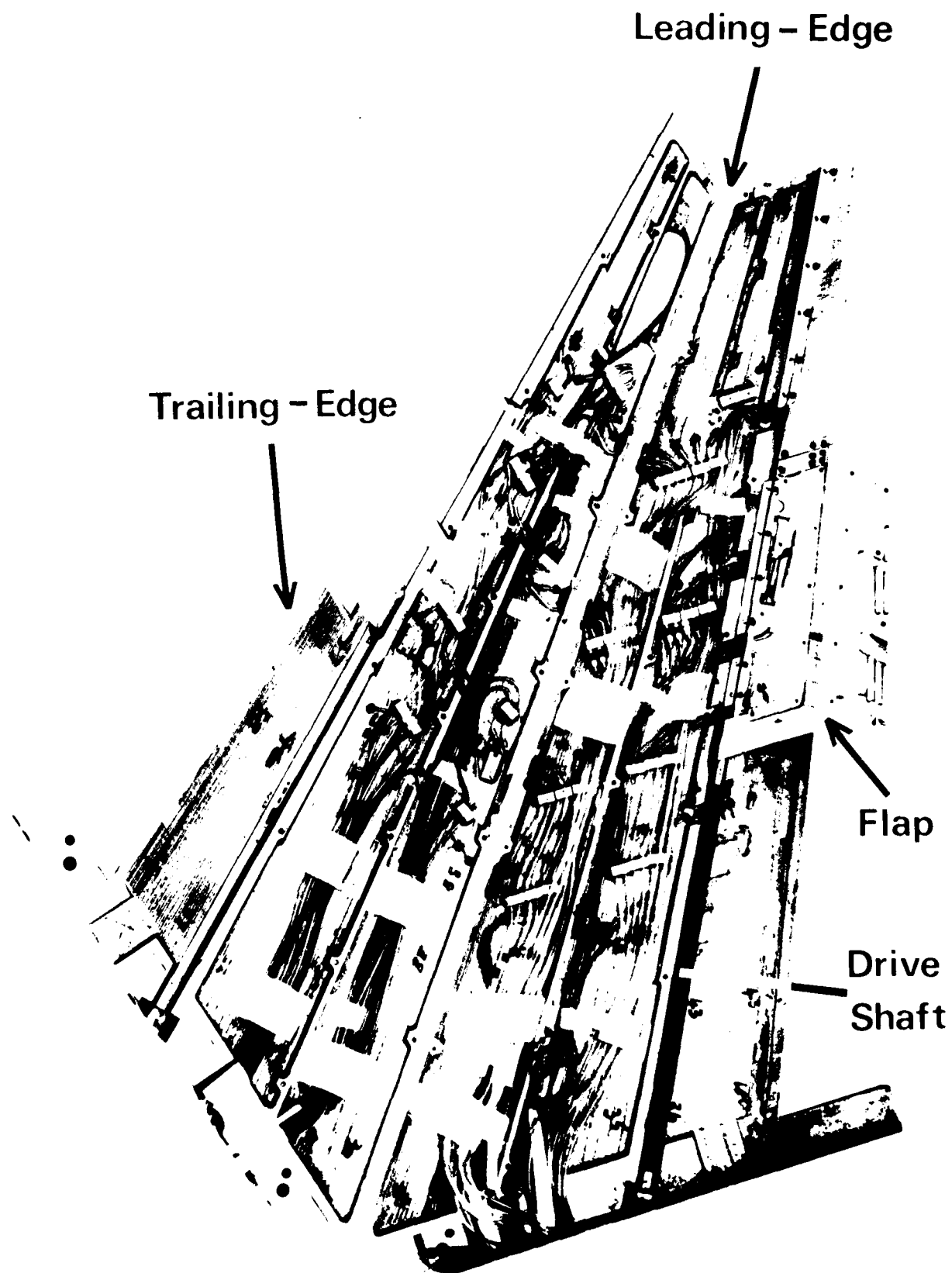
TM Str 947   C15605

Fig 5   Model assembly

Fig. 6

STATIC PRESSURE DISTRIBUTION

$\eta = 0.35$
$Rc_0 = 2.0 \times 10^6$

Measured

Calculated

$-C_p$

2D - FLAT PLATE

$M = 0.40$
$x/c = 0.70$
$\alpha = 0^0$

Calculations		
η	x_t/c	
	0.125	0.250
0.28	⊙	▣
0.80	×	+

$10^3 C_f$

$R\delta_1$
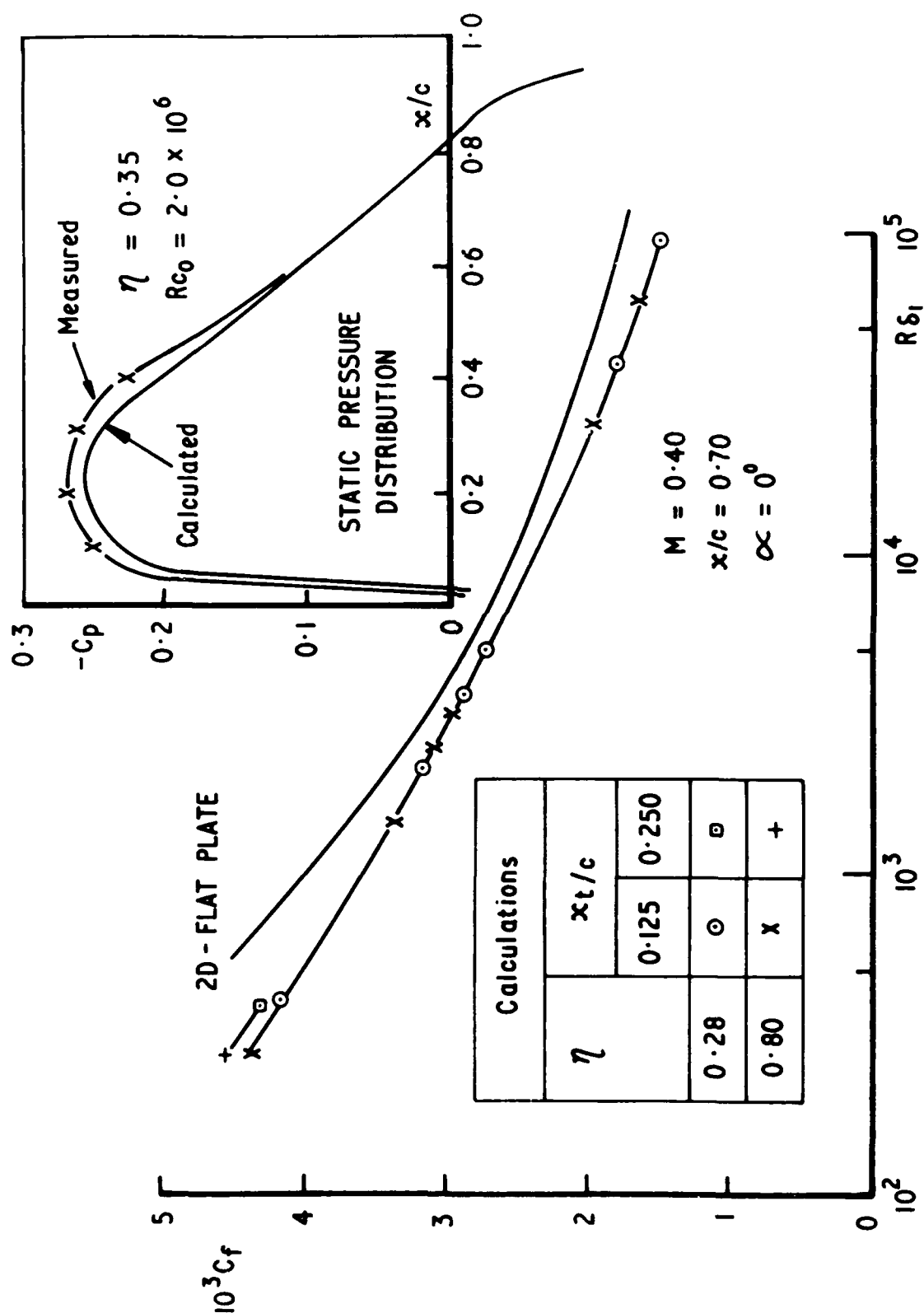
Fig. 6   Calculated Skin Friction Coefficient v Displacement Thickness Reynolds Number

Fig. 7

(a) M = 0.80

(b) M = 0.90
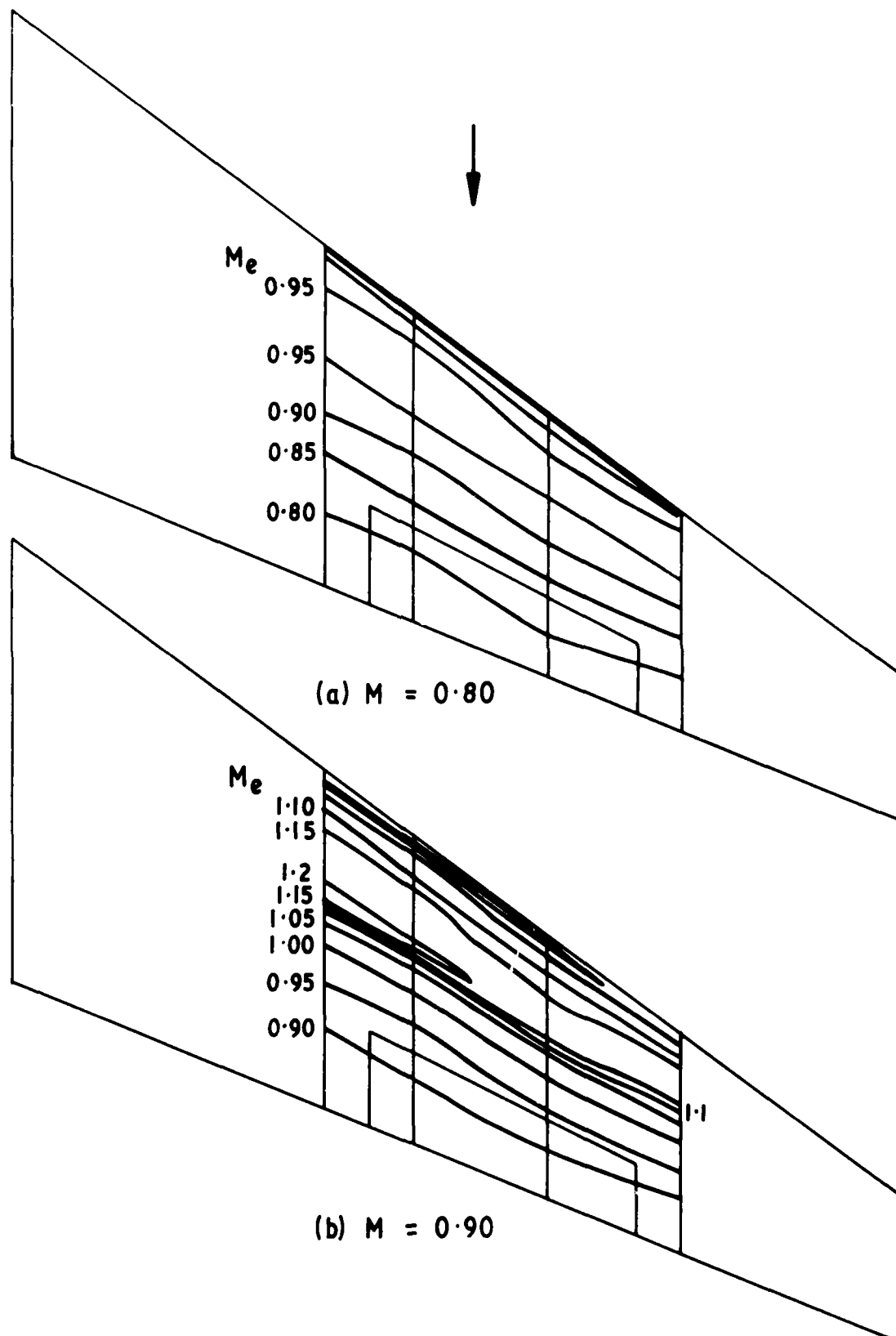
Fig. 7   Contours of Local Mach Number ($\alpha = 0^0$)

Fig. 8

$\eta = 0.35$

$\eta = 0.45$

M = 0.80
TRANSITION FIXED
$r = 0.35$
$f = 90Hz$

$\eta = 0.60$

Theory

Experiment

$\eta = 0.75$
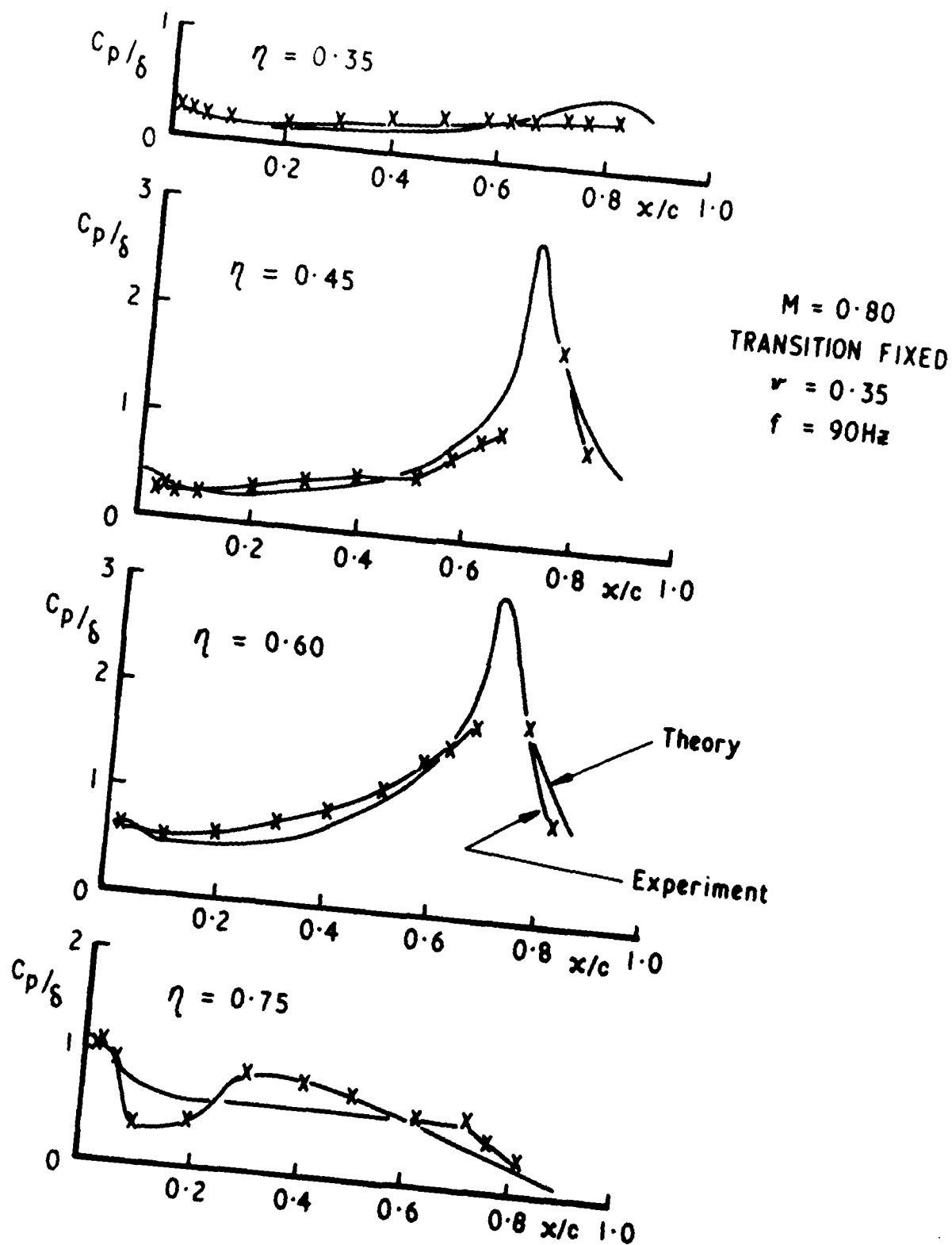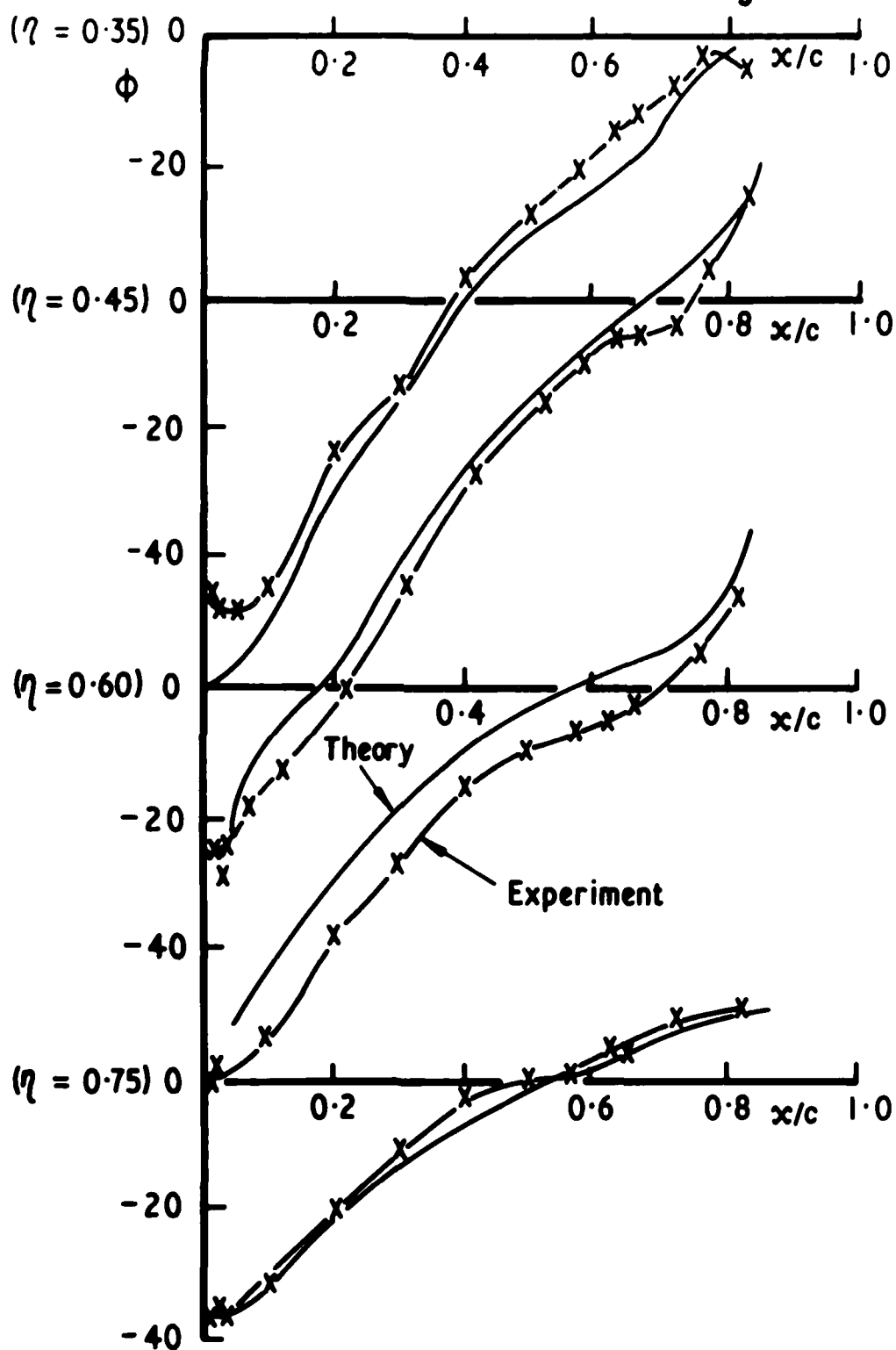
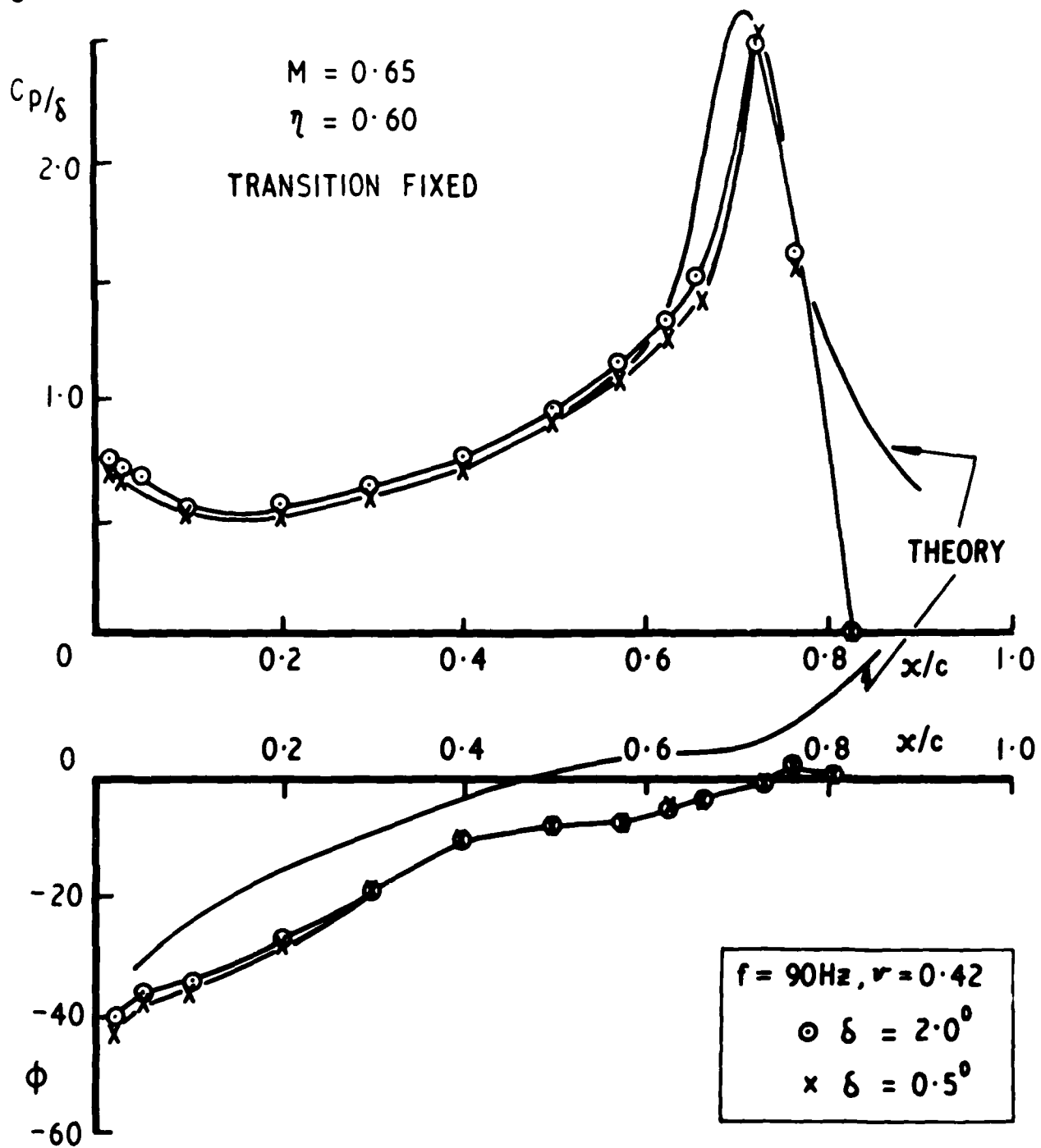8(a)   MAGNITUDE

Fig. 8 Pressure Distributions at Four
Spanwise Stations

Fig. 8 cncld.

8 (b) PHASE

Fig. 8 cncld. Pressure Distributions at Four
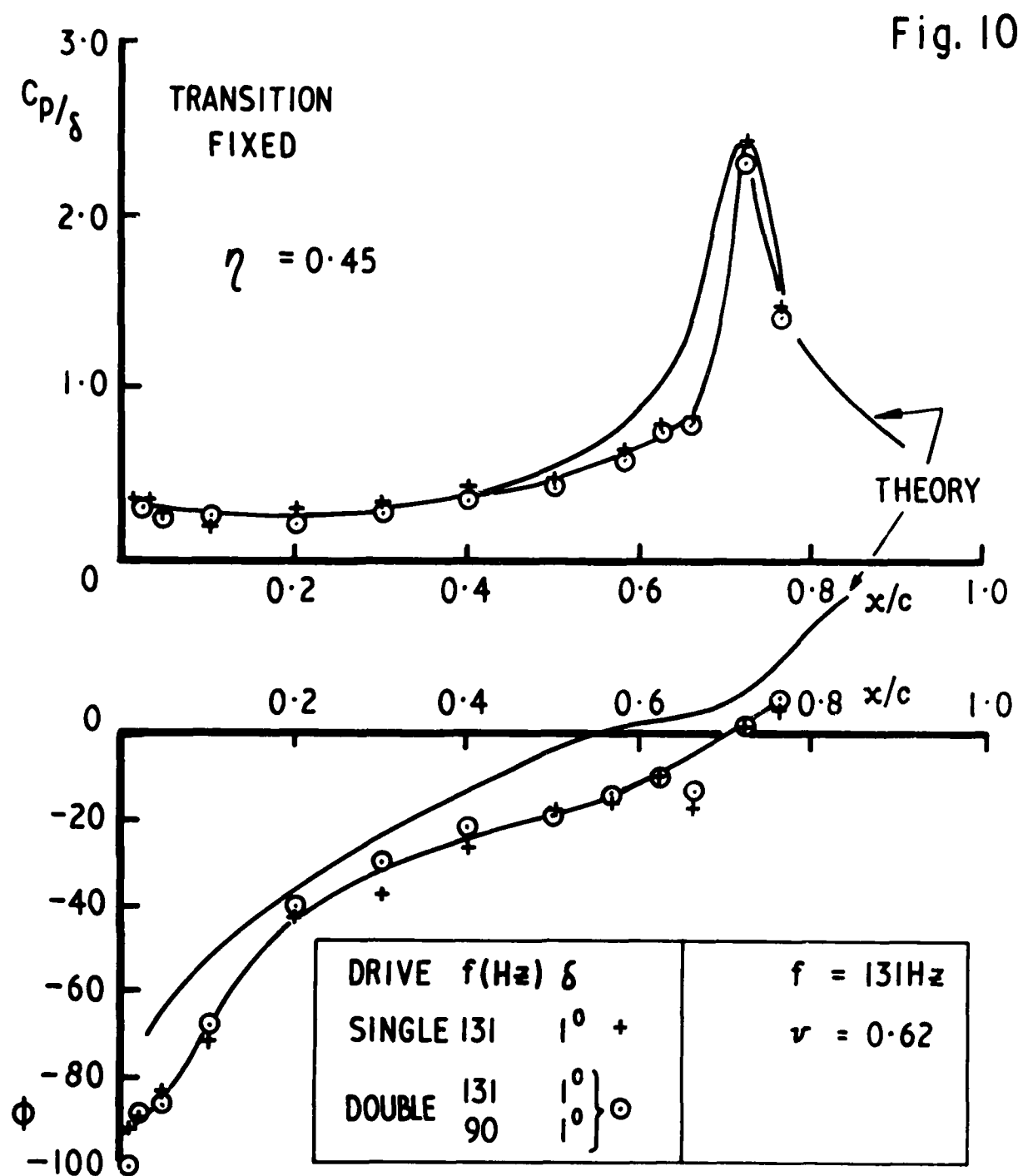Spanwise Stations

Fig. 9   Effect of Varying Amplitude

Fig. 10

TRANSITION FIXED

$\eta = 0.45$

THEORY

DRIVE	f(Hz)	δ	
SINGLE	131	1^0	+
DOUBLE	131	1^0	$\odot$
	90	1^0	

$f = 131 Hz$

$v = 0.62$

10(a)   SUBSONIC   M = 0.65

Fig. 10   Superposition of Two Frequencies

T Memo Struct 947

Fig. 10 cncld.

TRANSITION FIXED

$Rc_0 = 3 \cdot 3 \times 10^6$

$\eta = 0 \cdot 45$

DRIVE	f(Hz)	δ		$f = 131Hz$
SINGLE	131	1^0 +		$r = 0 \cdot 47$
DOUBLE	131 90	$\left.\begin{matrix}1^0\\1^0\end{matrix}\right\}$ ⊙		
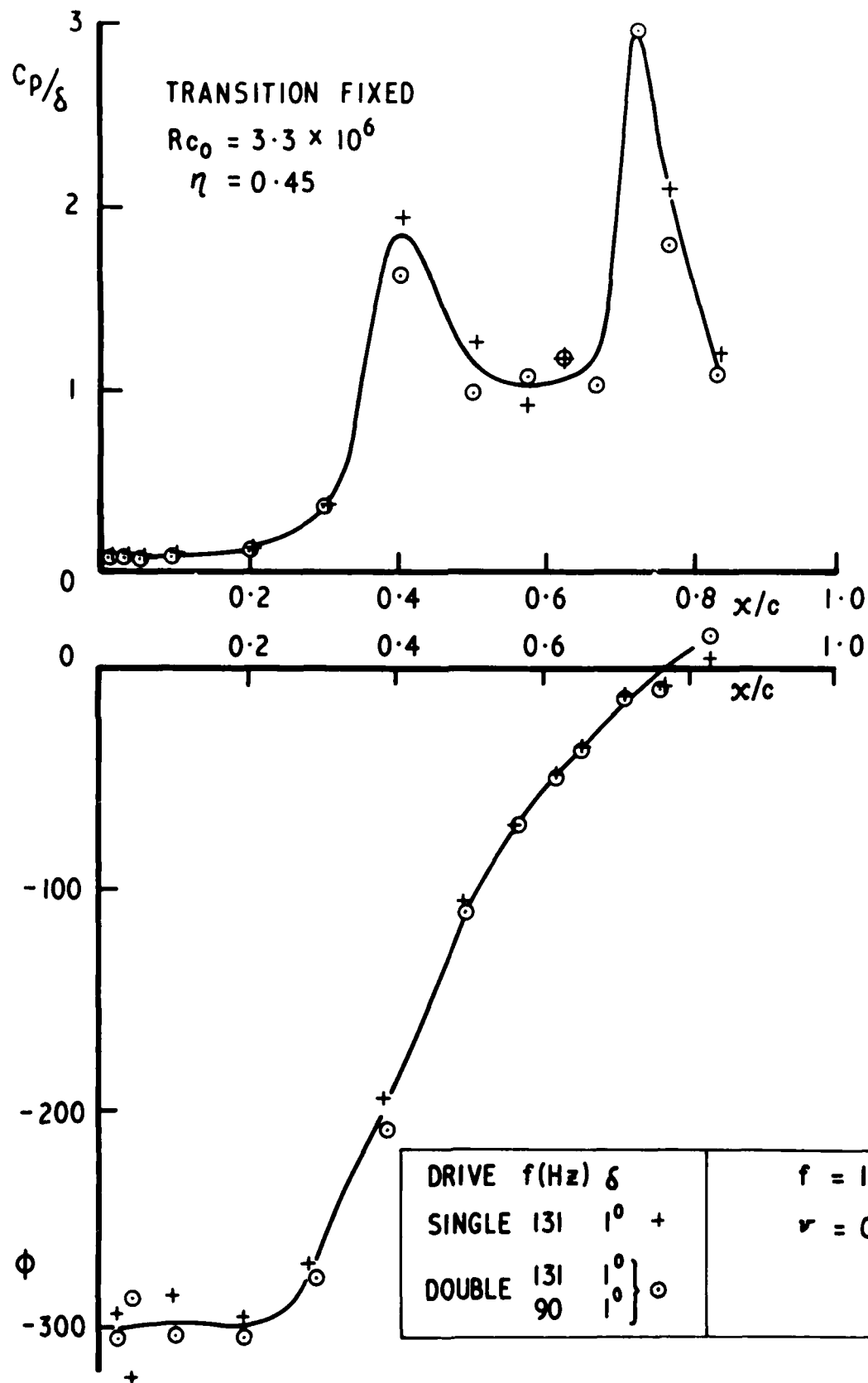
10 (b)   TRANSONIC   M = 0·90

Fig.10 cncld. Superposition of Two Frequencies

Fig. 11

(a) M = 0·80

TRANSITION FREE

(b) M = 0·90
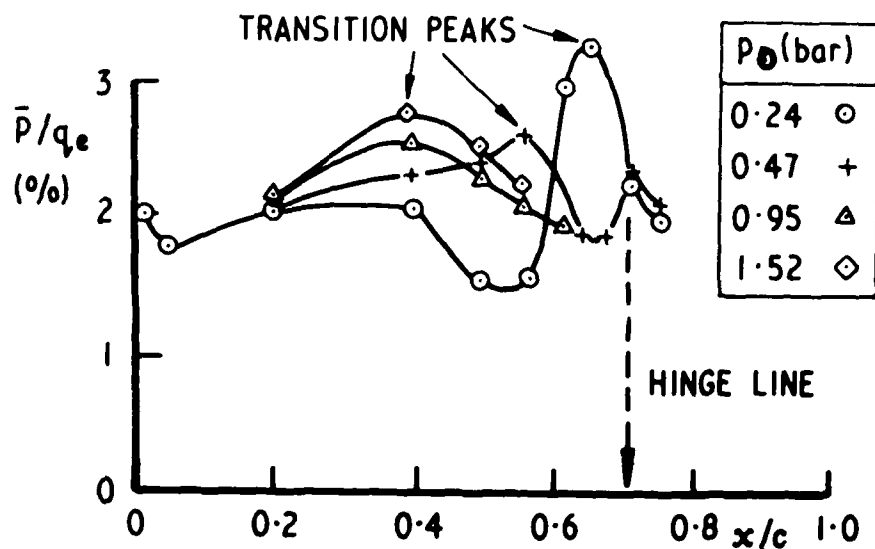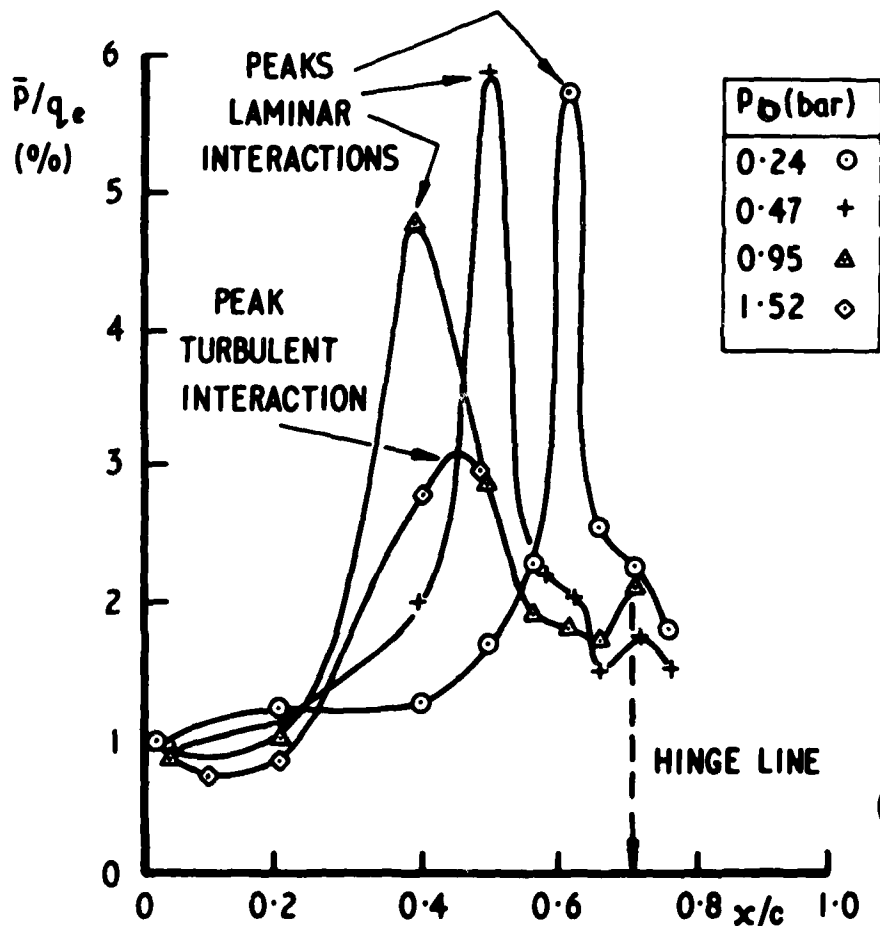
RMS PRESSURE FLUCTUATIONS v CHORDWISE STATION
(FLAP – UNDRIVEN)

Fig. 11   Transition Determination at $\eta = 0\cdot60$ ($\alpha = 0^{0}$)
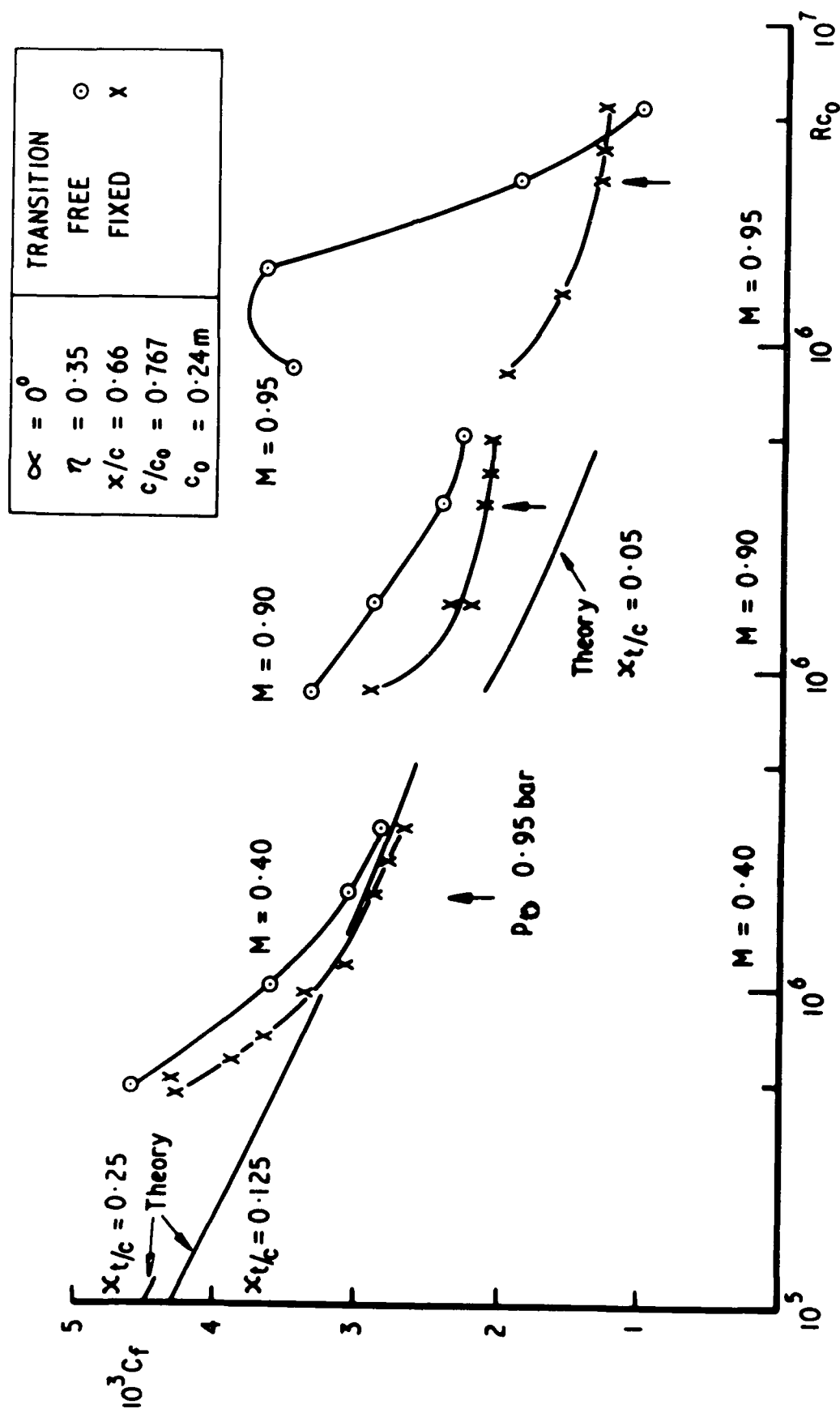
T Memo Struct 947

Fig. 12

Fig.12 Skin Friction Coefficients near Hinge Line

T Memo Struct 947
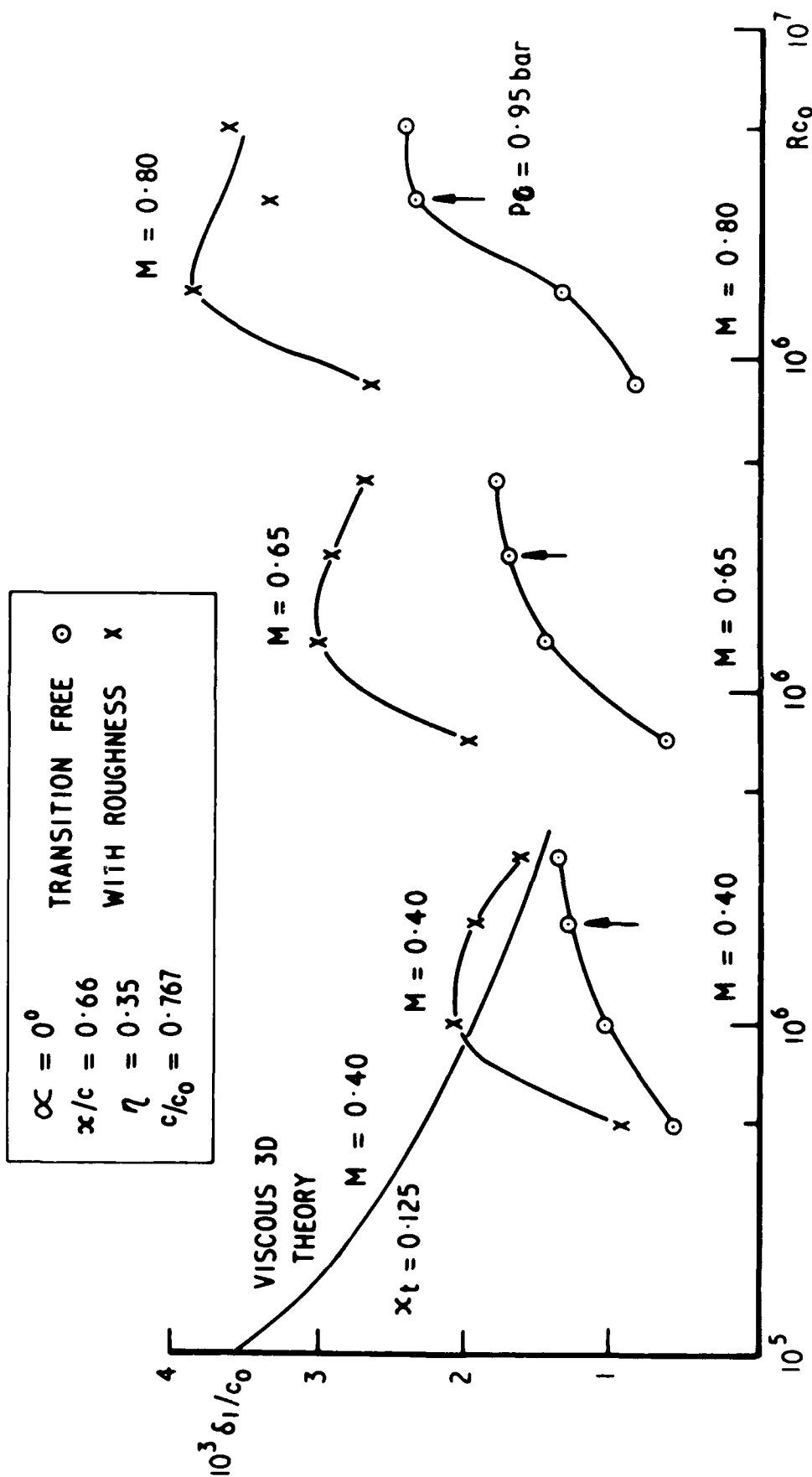
Fig. 13 Variation of Boundary Layer Displacement Thickness with Mach Number and Reynolds Number
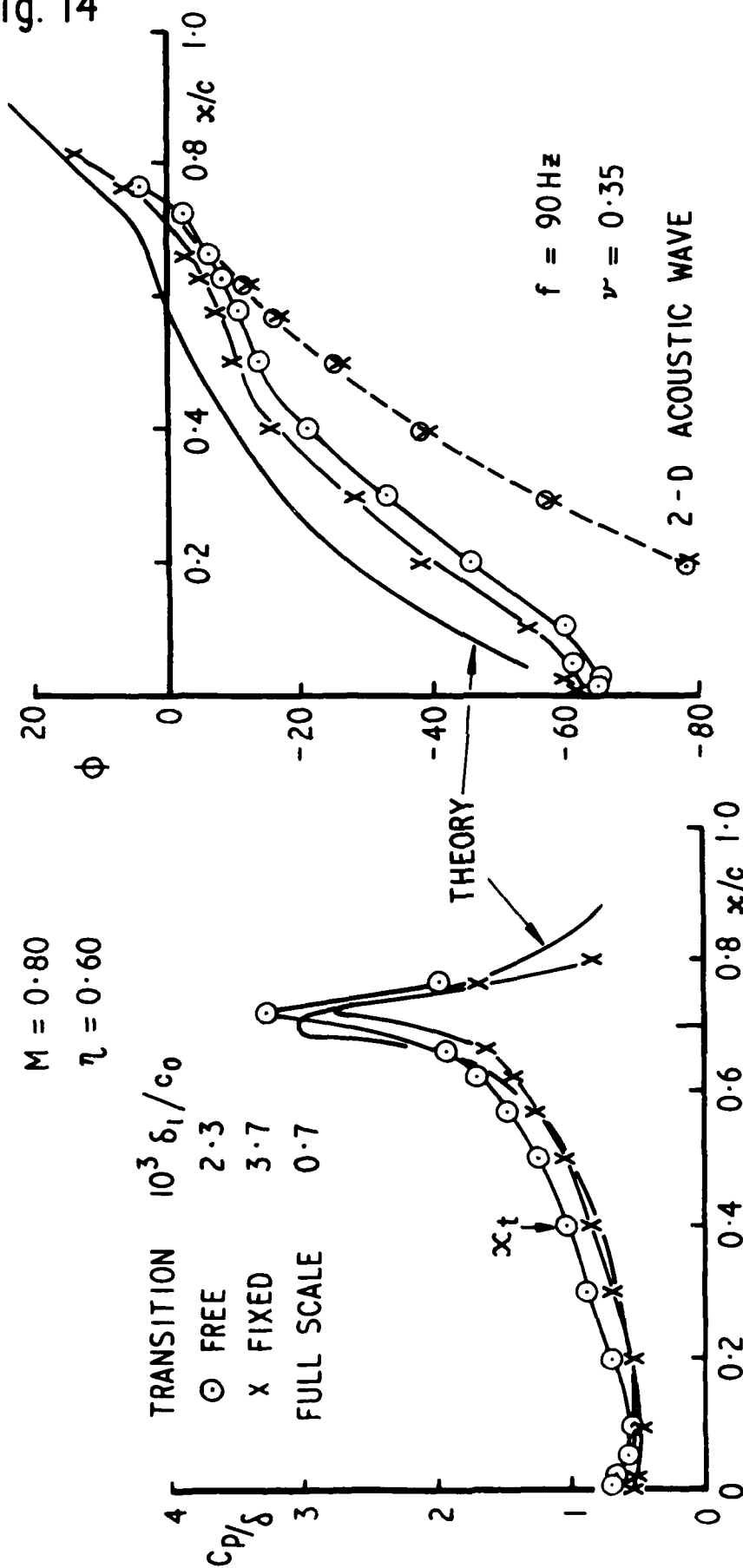
Fig. 14

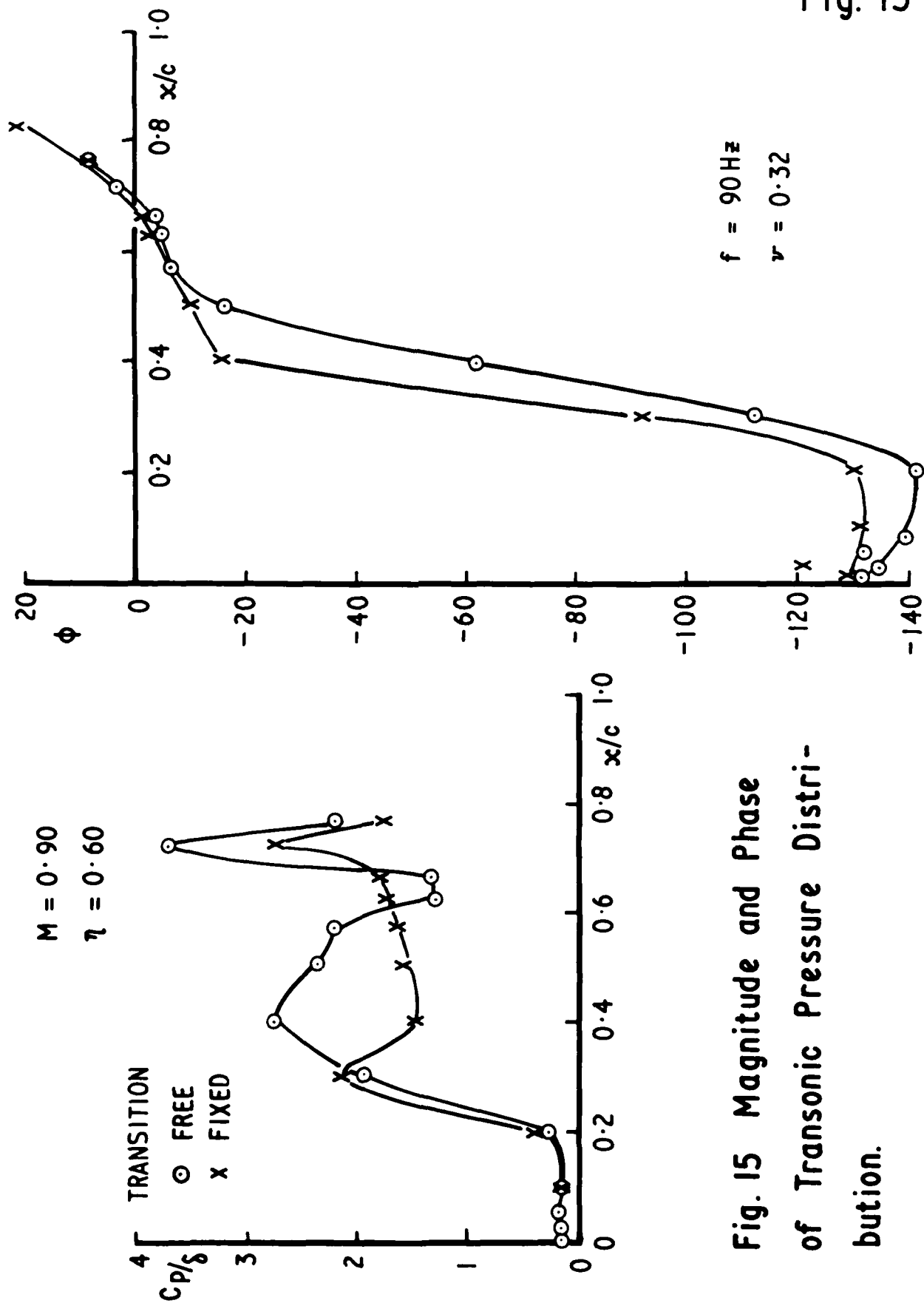Fig. 14 Magnitude and Phase of Subsonic Pressure Distribution

Fig. 15

f = 90 Hz

ν = 0.32

M = 0·90

η = 0·60

TRANSITION
⊙ FREE
× FIXED

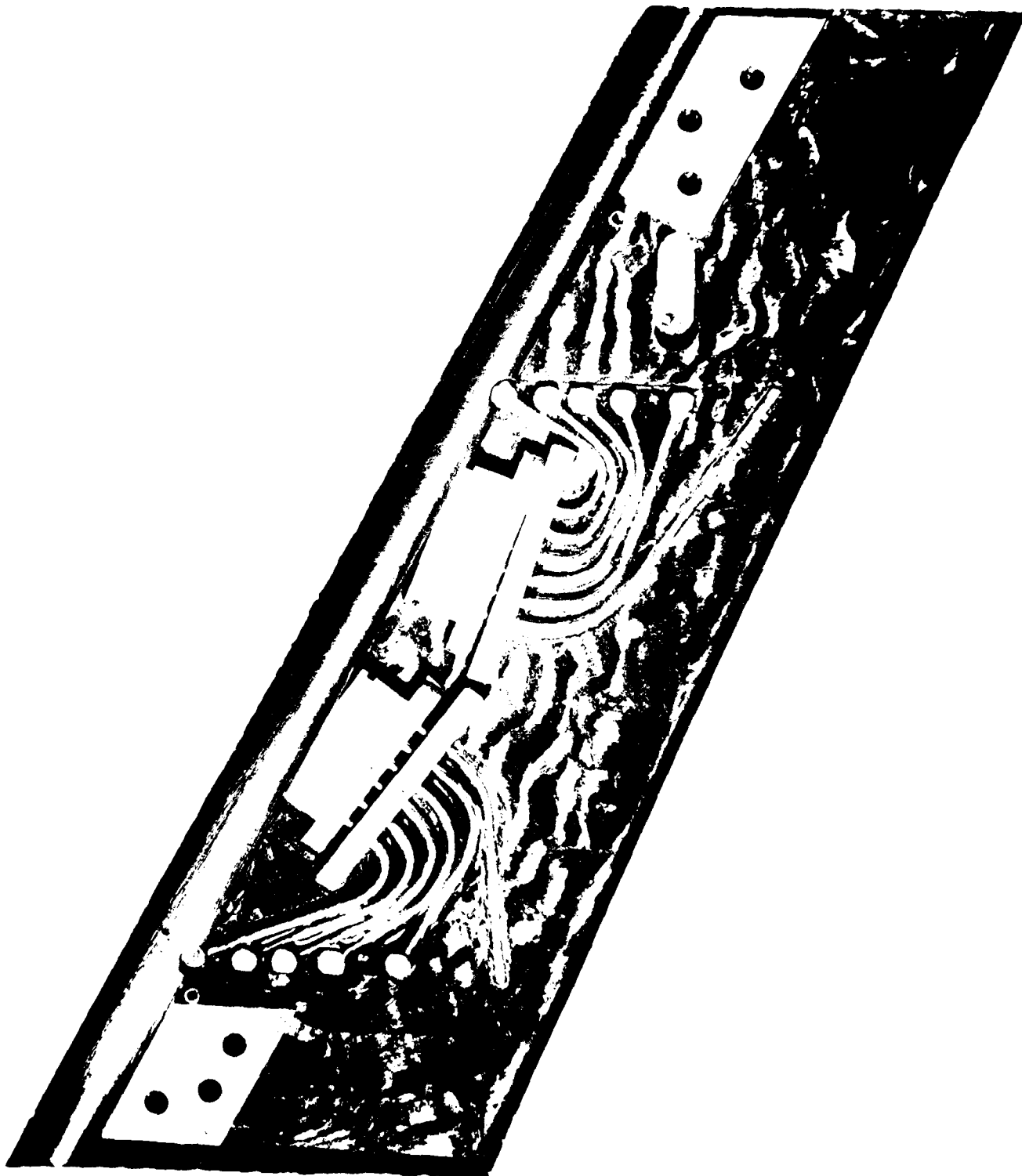Fig. 15 Magnitude and Phase of Transonic Pressure Distribution.

Fig 16

Fig 16   New flap

bQ bb A085033   (U)   FIELD/GROUP bbbbbb

UNCLASSIFIED TITLE
    AERODYNAMIC CHARACTERISTICS OF MOVING TRAILING-EDGE CONTROLS AT SUBSO

ABSTRACT
    (U)   THIS PAPER COMPARES OSCILLATORY PRESSURES CALCULATED AND MEASURE
    ASPECT RATIO 6 WITH A PART-SCAN TRAILING-EDGE FLAP. THE FLAP WAS DRI
    Z AT MACH NUMBERS FROM 0.40 TO 0.95 WITH BOTH FIXED AND FREE TRANSITI
    TO 4 MILLION. THE MEASURED OSCILLATORY PRESSURES DEPEND STRONGLY ON
    INGE LINE. HENCE EXTRAPOLATION FROM MODEL TO FULL SCALE REQUIRES GREA
    UN GIVE THE THINNEST TURBULENT BOUNDARY LAYER AT THE HINGE LINE AND C
    PEEDS TRANSITION SHOULD BE FIXED AT A SAFE DISTANCE UP-STREAM OF THE
    RESULTS APPROPRIATE TO HIGHER REYNOLDS NUMBER. TESTS WITH FLAP DRIVE
    HZ) AT SUBSONIC AND TRANSONIC SPEEDS PRODUCE THE SAME OSCILLATORY PR
    NCE THE PRINCIPLE OF SUPERPOSITION APPLIES, AT LEAST FOR SMALL AMPLIT

INDEX TERMS ASSIGNE

AERODYNAMIC CHARACTERISTICS   TRANSITIO
HIGH VELOCITY   SUBSONIC
REYNOLDS NUMBER   MACH NUMB
OSCILLATION   PRESSURE
REYNOLDS NUMBER   AMPLITUDE
MOTION   SUBSONIC
SUBSONIC CHARACTERISTICS   VELOCITY
TRANSONIC CHARACTERISTICS   VELOCITY
TURBULENT BOUNDARY LAYER

TERMS NOT FOUND ON NL

ASPECT RATIO 6   ATTACHED
BOUNDARY-LAYER DISPLACEMENT THICKNESS   FIXED TRA
FORWARD EXCURSION   FULL SCAL
GREAT CARE   HINGE LIN
MOVING TRAILING-EDGE CONTROLS   PART-SCAN
QUASI-STEADY HZ   SAFE DIST
SWEPT BACK WING   TRANSONIC
1 HZ   131 HZ
90 HZ

@@@

ILING-EDGE CONTROLS AT SUBSONIC AND TRANSONIC SPEEDS.

SURFS CALCULATED AND MEASURED AT HIGH SUBSONIC SPEEDS FOR A SWEPT BACK WING OF
-EDGE FLAP. THE FLAP WAS DRIVEN AT FREQUENCIES OF 1 HZ (QUASI-STEADY) AND 90 H
BOTH FIXED AND FREE TRANSITION OVER A RANGE OF REYNOLDS NUMBERS FROM 1 MILLION
RESSURES DEPEND STRONGLY ON THE BOUNDARY-LAYER DISPLACEMENT THICKNESS AT THE M
TO FULL SCALE REQUIRES GREAT CARE. IN SUBSONIC FLOW, TESTS WITH FREE TRANSITI
AYER AT THE HINGE LINE AND COME NEAREST TO FULL SCALE. HOWEVER, AT TRANSONIC S
E DISTANCE UP-STREAM OF THE MOST FORWARD EXCURSION OF THE SHOCK WAVE TO OBTAIN
UMBER. TESTS WITH FLAP DRIVEN SIMULTANEOUSLY AT TWO FREQUENCIES (90 HZ AND 131
DUCE THE SAME OSCILLATORY PRESSURES AT 131 HZ AS WHEN DRIVEN INDEPENDENTLY. HE
S, AT LEAST FOR SMALL AMPLITUDE MOTIONS WITH ATTACHED FLOWS. (AUTHOR)

      INDEX TERMS ASSIGNED
           TRANSITIONS
           SUBSONIC FLIGHT
           MACH NUMBER
           PRESSURE
           AMPLITUDE
           SUBSONIC FLOW
           VELOCITY
           VELOCITY

      TERMS NOT FOUND ON NLDB
           ATTACHED FLOWS
           FIXED TRANSITION
           FULL SCALE
           HINGE LINE
           PART-SCAN TRAILING-EDGE FLAP
           SAFE DISTANCE UP-STREAM
           TRANSONIC SPEEDS TRANSITION
           131 HZ

REPORT DOCUMENTATION PAGE

Overall security classification of this page

UNLIMITED

As far as possible this page should contain only unclassified information. If it is necessary to enter classified information, the box above must be marked to indicate the classification, e.g. Restricted, Confidential or Secret.

1. DRIC Reference (to be added by DRIC)	2. Originator's Reference RAE TM Structures 947	3. Agency Reference N/A	4. Report Security Classification/Marking UNLIMITED

5. DRIC Code for Originator 7673000W	6. Originator (Corporate Author) Name and Location Royal Aircraft Establishment, Farnborough, Hants, UK

5a. Sponsoring Agency's Code N/A	6a. Sponsoring Agency (Contract Authority) Name and Location N/A

7. Title Aerodynamic characteristics of moving trailing-edge controls at subsonic and transonic speeds

7a. (For Translations) Title in Foreign Language

7b. (For Conference Papers) Title, Place and Date of Conference
Paper prepared for AGARD Symposium on Aerodynamic Characteristics of Controls, Naples, May 1979

8. Author 1. Surname, Initials Mabey, D.G.	9a. Author 2 McOwat, D.M.	9b. Authors 3, 4 .... Welsh, B.L.	10. Date June 1979	Pages 28	Refs. 17

11. Contract Number N/A	12. Period N/A	13. Project	14. Other Reference Nos.

15. Distribution statement
    (a) Controlled by —

    (b) Special limitations (if any) —

16. Descriptors (Keywords)   (Descriptors marked * are selected from TEST)

Unsteady aerodynamics.

17. Abstract

This paper compares oscillatory pressures calculated and measured at high subsonic speeds for a swept back wing of aspect ratio 6 with a part-span trailing-edge flap. The flap was driven at frequencies of 1 Hz (quasi-steady) and 90 Hz at Mach numbers from 0.40 to 0.95 with both fixed and free transition over a range of Reynolds numbers from 10^6 to 4×10^6.

The measured oscillatory pressures depend strongly on the boundary layer displacement thickness at the hinge line. Hence extrapolation from model to full scale requires great care. In subsonic flow, tests with free transition give the thinnest turbulent boundary layer at the hinge line and come nearest to full scale. However, at transonic speeds transition should be fixed at a safe distance upstream of the most forward excursion of the shock wave to obtain results appropriate to higher Reynolds number.

Tests with flap driven simultaneously at two frequencies (90 Hz and 131 Hz) at subsonic and transonic speeds produce the same oscillatory pressures at 131 Hz as when driven independently. Hence the principle of superposition applies, at least for small amplitude motions with attached flows.